

1 **TITLE**

2 Endemic, endangered, and evolutionarily significant: Cryptic lineages in Seychelles' frogs  
3 (Anura: Sooglossidae).

4 **RUNNING TITLE**

5 Cryptic diversity in the Sooglossidae

6 **AUTHORS**

7 **Jim Labisko (corresponding author – jl693@kent.ac.uk)**

8 Durrell Institute of Conservation and Ecology, School of Anthropology and Conservation,  
9 University of Kent, Canterbury, Kent. CT2 7NR. UK; Island Biodiversity and Conservation, P.O.  
10 Box 1348, Anse Royale, Mahé, Seychelles.

11 **Richard A. Griffiths**

12 Durrell Institute of Conservation and Ecology, School of Anthropology and Conservation,  
13 University of Kent, Canterbury, Kent. CT2 7NR. UK.

14 **Lindsay Chong-Seng**

15 Plant Conservation Action group, P.O. Box 392, Victoria, Mahé, Seychelles.

16 **Nancy Bunbury**

17 Seychelles Islands Foundation, La Ciotat Building, Mont Fleuri. P.O. Box 853, Victoria, Mahé,  
18 Seychelles; Centre for Ecology and Conservation, University of Exeter, Cornwall Campus,  
19 Penryn, TR10 9FE, UK.

20 **Simon T. Maddock**

21 School of Biology, Chemistry and Forensic Science, Faculty of Science and Engineering,  
22 University of Wolverhampton, Wulfruna Street, Wolverhampton. WV1 1LY. UK; Department  
23 of Life Sciences, The Natural History Museum, Cromwell Road, London. SW7 5BD. UK;  
24 Department of Genetics, Evolution and Environment, University College London, Gower

25 Street, London. WC1E 6BT. UK.; Island Biodiversity and Conservation, P.O. Box 1348, Anse  
26 Royale, Mahé, Seychelles.

27 **Kay S. Bradfield**

28 Perth Zoo, South Perth, WA 6151, Australia.

29 **Michelle L. Taylor**

30 Durrell Institute of Conservation and Ecology, School of Anthropology and Conservation,  
31 University of Kent, Canterbury, Kent. CT2 7NR. UK.

32 **Jim J. Groombridge**

33 Durrell Institute of Conservation and Ecology, School of Anthropology and Conservation,  
34 University of Kent, Canterbury, Kent. CT2 7NR. UK.

**35 ABSTRACT**

36 Cryptic diversity that corresponds with island origin has been previously reported in the  
37 endemic, geographically restricted sooglossid frogs of the Seychelles archipelago. The  
38 evolutionary pattern has not been fully explored, and given current amphibian declines and  
39 the increased extinction risk faced by island species, we sought to identify evolutionarily  
40 significant units (ESUs) to address conservation concerns for these highly threatened anurans.  
41 We obtained genetic data for two mitochondrial (mtDNA) and four nuclear (nuDNA) genes  
42 from all known populations of sooglossid frog (the islands of Mahé, Praslin, and Silhouette)  
43 to perform phylogenetic analyses and construct nuDNA haplotype networks. Bayesian and  
44 maximum likelihood analyses of mtDNA support monophyly and molecular differentiation of  
45 populations in all species that occur on multiple islands. Haplotype networks using statistical  
46 parsimony revealed multiple high-frequency haplotypes shared between islands and taxa, in  
47 addition to numerous geographically distinct (island-specific) haplotypes for each species. We  
48 consider each island-specific population of sooglossid frog as an ESU and advise conservation  
49 managers to do likewise. Furthermore, our results identify each island lineage as a candidate  
50 species, evidence for which is supported by Bayesian Poisson Tree Processes analyses of  
51 mtDNA, and independent analyses of mtDNA and nuDNA using the multispecies coalescent.  
52 Our findings add to the growing understanding of the biogeography and hidden diversity  
53 within this globally important region.

54

**55 Keywords**

56 Candidate species – cryptic diversity – evolutionarily significant unit – Indian Ocean – insular  
57 amphibians – islands – *Sechellophryne* – Seychelles – Sooglossidae – *Sooglossus*

## 58 INTRODUCTION

59 From the observations of Darwin (1859) and Wallace (1869) on the Galapagos and Malay  
60 archipelagos, to MacArthur and Wilson's (1967) seminal work on the theory of island  
61 biogeography, islands have played a significant role as model biological systems, progressing  
62 our understanding of evolutionary theory, ecological processes, and biogeography (Adseren,  
63 1995; Warren *et al.*, 2015; Santos *et al.*, 2016). The uniqueness of island endemic species is  
64 well documented, yet island biotas are particularly vulnerable to extinction, largely due to  
65 human-driven habitat change or introduced species (Paulay, 1994; Cronk, 1997; Whittaker &  
66 Fernández-Palacios, 2007). Understanding the evolutionary relationships of insular taxa, and  
67 addressing threats to endemic island lineages are therefore key components in mitigating the  
68 loss of global biodiversity (Robertson *et al.*, 2014).

69 The granitic Seychelles (most of the inner islands of the group; Fig. 1) form part of an  
70 isolated continental block with mixed faunal origins, including both overwater dispersed and  
71 ancient endemic clades (Ali, 2017; Ali, 2018) that reveal varying degrees of affinity to the  
72 Afrotropical and Indomalayan realms. Recent explorations of molecular phylogenetic  
73 relationships of Seychelles herpetofauna have identified a broad partitioning of two  
74 biogeographic units; a northern group (consisting of Praslin and surrounding islands) and a  
75 southern group (comprised of Mahé, Silhouette, and surrounding islands) (Fig. 1). This pattern  
76 of differentiation is documented in studies across a range of taxa, including the geckos  
77 *Ailuronyx* (Rocha *et al.*, 2016a), *Phelsuma* (Rocha *et al.*, 2013), *Urocotyledon* (Rocha *et al.*,  
78 2011); and the skinks *Pamelaescincus* (Valente *et al.*, 2013) and *Trachylepis* (formerly  
79 *Mabuya*) (Rocha *et al.*, 2016b). However, within this north-south biogeographic pattern,  
80 further evidence of cryptic diversity is beginning to emerge in several taxa (e.g. Rocha *et al.*,  
81 2016b). The discovery of a previously unknown population of sooglossid frogs on the island

82 of Praslin—where the frogs had hitherto been unrecorded—and identification of this  
83 population as an evolutionarily significant unit (ESU) (Taylor *et al.*, 2012) provided the  
84 motivation to assess the genetic diversity of this family.

85

## 86 **Sooglossid frogs**

87 One of the world’s most enigmatic and understudied frog families, the Sooglossidae (Noble,  
88 1931) is one of only two amphibian families entirely restricted to an archipelago. Comprised  
89 of two genera, each with two species: *Sooglossus sechellensis* (Boettger, 1896) and *So.*  
90 *thomasseti* (Boulenger, 1909), and *Sechellophryne gardineri* (Boulenger, 1911) and *Se.*  
91 *pipilodryas* (Gerlach & Willi, 2002), each are recognised as Evolutionarily Distinct and Globally  
92 Endangered (EDGE) species and are placed in the Top 100 EDGE Amphibians (Isaac *et al.*,  
93 2012; Zoological Society of London, 2015), and have been assessed for the IUCN Red List as  
94 either Critically Endangered (*So. thomasseti*, *Se. pipilodryas*) or Endangered (*So. sechellensis*,  
95 *Se. gardineri*) (IUCN SSC Amphibian Specialist Group, 2013a; IUCN SSC Amphibian Specialist  
96 Group, 2013b; IUCN SSC Amphibian Specialist Group, 2013c; IUCN SSC Amphibian Specialist  
97 Group, 2013d). Three of the four species occur on more than one island, with *So. thomasseti*  
98 and *Se. gardineri* found on Mahé and Silhouette (Nussbaum, 1984), and *So. sechellensis* found  
99 on Mahé, Silhouette, and Praslin (Nussbaum, 1984; Taylor *et al.*, 2012). The fourth species,  
100 *Se. pipilodryas*, is endemic to Silhouette (Gerlach & Willi, 2002).

101         Given the (i) importance of maintaining global and regional biological diversity, (ii)  
102 increased extinction risk faced by island species, (iii) unabated international crisis of  
103 amphibian declines, and (iv) global significance of the Sooglossidae as an evolutionarily  
104 distinct group, this unique family is in urgent need of research attention. A stronger  
105 knowledge base is also essential for conservation practitioners to make informed decisions

106 and manage the sooglossid populations. Following recent accounts of geographic partitioning  
107 in Seychelles herpetofauna, and the identification of a novel, evolutionarily distinct  
108 population of sooglossid frogs on Praslin, we hypothesise that: (1) undocumented cryptic  
109 diversity exists across the three islands where these sooglossids occur, and (2) identification  
110 of such diversity will correspond with biogeographic (island) origin. To test these hypotheses,  
111 we reconstructed mitochondrial DNA phylogenies to explore the presence of divergent,  
112 cryptic lineages; generated nuclear DNA haplotype networks to reveal phylogeographic  
113 relationships; and performed species tree reconstructions using the multispecies coalescent.  
114 Our results enable the identification of ESUs for conservation purposes (Moritz, 1994) and  
115 further our understanding of the biogeography of the region.

116

## 117 **MATERIALS AND METHODS**

### 118 **Study site**

119 The inner islands of the Seychelles archipelago lie 4-5°S to 55-56°E in the western Indian  
120 Ocean, and sit upon the Seychelles Bank, a largely submerged microcontinent of some  
121 129,500 km<sup>2</sup> (Davies & Francis, 1964). Its flat upper section spans ca. 44,000 km<sup>2</sup> and lies an  
122 average depth of 55 m below present sea level (bpsl), emerging from which are the granitic  
123 inner islands (Davies & Francis, 1964; Matthews & Davies, 1966; Ali, 2018) (Fig. 1). The granitic  
124 Seychelles are unique among oceanic islands, being composed of continental rock, and  
125 formed upon separation from India ~63 Ma (Collier *et al.*, 2008; Chatterjee *et al.*, 2013).  
126 Elevated, forested areas on the largest and highest islands of Mahé (154 km<sup>2</sup>, 905 m  
127 elevation), Praslin (38 km<sup>2</sup>, 367 m elevation) and Silhouette (20 km<sup>2</sup>, 740 m elevation) are the  
128 only locations where sooglossid frogs are found.

129

## 130 **Genetic sampling**

131 Non-lethal tissue samples (toe-clips) were obtained from frogs representing each species and  
132 island population (Fig. 1; Table 1). We sequenced genes regularly utilised in amphibian  
133 phylogenetics that represented varying rates of molecular evolution. These comprised two  
134 mitochondrial DNA (mtDNA) fragments: *16S* rRNA (*16s*) and cytochrome b (*cytb*), plus  
135 fragments of four nuclear loci (nuDNA): proopiomelanocortin (*pomc*), recombination  
136 activating genes (*rag*) 1 and 2, and rhodopsin exon 1 (*rho*). Genomic DNA was extracted  
137 following manufacturer's guidelines using the Bioline Isolate Genomic DNA Kit. Sequences  
138 from all loci were amplified via standard polymerase-chain reaction (PCR). For primers and  
139 cycling conditions see Appendix S1; Table S1.1 in Supporting Information. Products from PCR  
140 were sequenced by Macrogen, Korea. We also utilised GenBank sequence data arising from  
141 Taylor *et al.* (2012) (*So. sechellensis 16s*), van der Meijden *et al.* (2007) (*Se. pipilodryas 16s*,  
142 *rag1*, *rag2*), and for outgroups used in phylogenetic analyses (Table S1.2). Novel sequence  
143 data generated by this study have been submitted to GenBank under accession numbers  
144 MK058722-70; MK058781-823; MK058825-979; MK058996-9390; MK072763-5.

145

## 146 **Sequence alignment**

147 Sequences were quality trimmed in SEQUENCHER v. 5.3 (Gene Codes Corporation, 2015) and  
148 cross-checked with chromatograms by eye in MEGA6 (Tamura *et al.*, 2013). MEGA6 was also  
149 employed to visually check (e.g. for stop codons and indels), edit, and align sequence data  
150 using default settings of the MUSCLE algorithm (Edgar, 2004). To remove any ambiguously  
151 aligned regions, sequence profiles were prepared via the GBLOCKS server v. 0.91b  
152 (Castresana, 2000; Talavera & Castresana, 2007). To preserve informative insertions and/or  
153 deletions, GBLOCKS parameters were set to allow gaps and less stringent flanking positions.

154 DATACONVERT 1.0 (Dyer *et al.*, n.d.), ALTER (Glez-Pena *et al.*, 2010) and FORMAT CONVERTOR  
155 (Los Alamos National Security LLC, 2005-2006) were employed to convert sequence profiles  
156 between required formats. SEQUENCEMATRIX v. 1.7.8 (Vaidya *et al.*, 2011) was used to  
157 concatenate mtDNA sequence profiles.

158

### 159 **Mitochondrial phylogeny**

160 Sooglossid mtDNA sequences were analysed using Bayesian inference (BI) (Huelsenbeck *et*  
161 *al.*, 2001) and maximum likelihood (ML) (Felsenstein, 1981) approaches. Partitioning schemes  
162 and models of nucleotide evolution were determined independently with PARTITIONFINDER  
163 v. 1.1.1 (Lanfear *et al.*, 2012) (Table S1.3). Branch lengths of alternative partitions were linked  
164 and all schemes evaluated using the Akaike information criterion. Bayesian analysis was  
165 performed in BEAST v. 2.3.2 (Bouckaert *et al.*, 2014) using two independent Markov chains of  
166 100 million generations, sampling every 10,000 generations. BEAST input files were generated  
167 using BEAUTI v. 2.3.2 (Bouckaert *et al.*, 2014). Chain convergence and all parameters were  
168 checked using TRACER v. 1.6 (Rambaut *et al.*, 2014) to ensure adequate mixing and effective  
169 sample size (ESS) values  $\geq 200$ . Initial runs were used to fine-tune final analyses, and we  
170 employed a relaxed lognormal clock as this approach may more accurately reflect lineage-  
171 and locus-specific heterogeneity in rates of molecular evolution (Drummond *et al.*, 2006;  
172 Lepage *et al.*, 2007; Heled & Drummond, 2010). As BEAST uses a molecular clock to estimate  
173 the root position, no outgroup taxa were used in BI analyses (Heled & Drummond, 2010). We  
174 assumed a stable environment for the Sooglossidae over recent geological time, and  
175 therefore applied a constant population for tree priors. However, given our inter- and  
176 intraspecific sampling we also performed phylogenetic reconstruction using the Yule model  
177 tree prior. Support for internal branches was evaluated using Bayesian posterior probabilities



178 (PP), with well-supported clades indicated by PP values  $\geq 0.95$ . LOGCOMBINER v. 2.3.2  
179 (Bouckaert *et al.*, 2014) was used to combine tree files from the two independent runs, which  
180 was summarised as a single maximum clade credibility tree with mean PP values after a 10%  
181 burn-in using TREEANNOTATOR v. 1.8.2 (Drummond & Rambaut, 2007).

182 Maximum likelihood analyses were performed with RAXMLGUI v. 1.3.1 (Silvestro &  
183 Michalak, 2012; Stamatakis, 2014) using default settings with GTRGAMMA model parameters  
184 and 1,000 bootstrap replicates. Branch lengths were individually optimised for each partition.  
185 The Nasikabatrachidae have been hypothesised to be the closest extant relative of the  
186 Sooglossidae (Biju & Bossuyt, 2003; Frost *et al.*, 2006; Roelants *et al.*, 2007; Pyron & Wiens,  
187 2011; Frazão *et al.*, 2015; Feng *et al.*, 2017) and used as an outgroup taxon in previous  
188 phylogenetic analyses of sooglossid frogs (van der Meijden *et al.*, 2007; Taylor *et al.*, 2012).  
189 However, GenBank derived *Nasikabatrachus sahyadrensis* sequence data rendered  
190 *Sooglossus* and *Sechellophryne* non-monophyletic in initial runs. Leiopelmatoidea  
191 (*Leiopelma*+*Ascaphus*) is widely accepted as the basal, sister lineage to all other extant  
192 anurans, and we therefore applied this taxon as an outgroup using GenBank sequence data  
193 arising from Irisarri *et al.* (2010) (*Leiopelma*) and Gissi *et al.* (2006) (*Ascaphus*). Support for  
194 internal branches was evaluated using bootstrap support (BS) values, with well-supported  
195 clades indicated by BS values  $\geq 70$ . Bayesian and maximum likelihood phylogenies were  
196 visualised using FIGTREE v. 1.4.3 (Rambaut, 2016).

197

### 198 **Multispecies coalescent and inference of population boundaries**

199 To infer underlying species trees and support a robust phylogenetic insight, we performed  
200 reconstructions using the multispecies coalescent applied in the StarBEAST (\*BEAST) package  
201 within BEAST v. 2.4.8 (Bouckaert *et al.*, 2014). Multiple samples per lineage are recommended

202 to infer coalescent events, speciation and topology (Heled & Drummond 2010; Jockusch *et*  
203 *al.*, 2014; Lambert *et al.*, 2015), therefore where possible we utilised composite taxa to  
204 achieve coverage where only a single representative of a lineage was available. Data for  
205 composites was derived from individuals arising from the same taxon and population of  
206 origin, thereby meeting previously published criteria for composite taxa in amphibian studies  
207 (e.g. Alonso *et al.*, 2012; Jockusch *et al.*, 2014; Maia-Carvalho *et al.*, 2014) (Table S1.4). The  
208 inclusion of variable loci such as mtDNA may exert disproportionate influence on other loci in  
209 \*BEAST analysis (Jockusch *et al.*, 2014). Accordingly, we carried out independent analyses of  
210 our mtDNA and nuDNA datasets. Partitioning schemes replicated that of our BEAST2 analyses  
211 (Table S1.3). Using a relaxed lognormal clock we ran two independent Markov chains of 100  
212 million generations, sampling every 1,000 generations, and applied the 'linear with constant  
213 root' multispecies coalescent prior with the Yule model distribution of prior probability.  
214 Mitochondrial DNA shared the same tree partition, nuDNA tree partitions were locus specific.  
215 Checks on chain convergence and ESS values were performed as previously described. Clade  
216 support was evaluated using PP values. Trees were visualised using FIGTREE.

217       To infer population boundaries and aid the identification of ESUs we subjected our  
218 BEAST2 mtDNA phylogeny to Bayesian Poisson Tree Processes (bPTP) analysis implemented  
219 via the online bPTP service (<http://species.h-its.org/ptp>) (Zhang *et al.*, 2013). The bPTP model  
220 applies two independent Poisson process classes (within- and among-species substitution  
221 events) under a coalescent model by assuming gene tree branch lengths to infer  
222 species/population boundaries. The bPTP analyses was run for 500 k Markov Chain Monte  
223 Carlo generations, with a thinning parameter of 100, and a burn-in of 0.1. Posterior  
224 probabilities of each node were assessed using maximum likelihood.

225

**226 Genetic variation**

227 MEGA6 was used to calculate nucleotide diversity, parsimony informative and variable sites,  
228 and obtain inter-and intra-specific genetic *p*-distances for mtDNA, with pair-wise deletion of  
229 missing sites. The PHASE algorithm (Stephens *et al.*, 2001; Stephens & Scheet, 2005)  
230 implemented in DNASP v. 5.10.1 (Librado & Rozas, 2009) was used to determine heterozygous  
231 positions and infer nuDNA haplotypes. Missing data can affect the success of haplotype  
232 phasing and detection of identical sequences (Salerno *et al.*, 2015), therefore short sequence  
233 reads were removed (*rag2*, *So. sechellensis*: Mahé = six, Praslin = two) and complete  
234 alignments for all nuDNA loci constructed. Random four-digit seeds generated by the TRUE  
235 RANDOM NUMBER SERVICE (Haahr, 2015) were applied to PHASE analyses which was run five  
236 times per locus with the highest pseudo-likelihood score used to select the best-fit model of  
237 haplotype estimation (Stephens & Donnelly, 2003). Heterozygous positions were deemed  
238 those achieving a score  $\geq 0.7$  (Harrigan *et al.*, 2008) and coded according to the International  
239 Union of Pure and Applied Chemistry. Remaining ambiguous positions were coded as 'N'. To  
240 check for saturation across codon positions, the test of Xia (Xia *et al.*, 2003) was applied using  
241 DAMBE v. 5.5.29 (Xia, 2013). To check for evidence of recombination, the DATAMONKEY  
242 software suite (Pond & Frost, 2005; Delpont *et al.*, 2010) was employed to select appropriate  
243 models and run analyses using the GARD application (Kosakovsky Pond *et al.*, 2006a;  
244 Kosakovsky Pond *et al.*, 2006b) under default settings. Haplotype networks were constructed  
245 using TCS v. 1.21 (Clement *et al.*, 2000) with a 95% connection limit and gaps treated as a fifth  
246 state. TCS networks were 'beautified' using TCSBU (Murias dos Santos *et al.*, 2016). Phased  
247 sequence data was used to infer haplotypes.

248 To detect evidence of historical population expansion or contraction in *So.*  
249 *sechellensis*, *So. thomasseti*, and *Se. gardineri* (*Se. pipilodryas* was excluded due to limited

250 sampling), we applied neutrality tests and performed skyline plots. Tajima's  $D$  (Tajima, 1989),  
251 Fu's  $F_S$  (Fu, 1997), and the  $R_2$  test statistic (Ramos-Onsins & Rozas, 2002) were run in DNASP  
252 v. 5.10.1 (Librado & Rozas, 2009) and applied to each locus individually. One thousand  
253 coalescent simulations were run for  $F_S$  and the  $R_2$  test. A conventional  $P$  value of 0.05 was  
254 adopted for Tajima's  $D$  and  $R_2$ ; Fu's  $F_S$  is interpreted as significant at  $P < 0.02$ . We performed  
255 Extended Bayesian Skyline plots (EBSP; Heled & Drummond, 2008) using unphased data for  
256 each island-specific population in BEAST v. 2.4.8 via the CIPRES Science Gateway (Miller *et al.*,  
257 2010). The Jeffrey's  $(1/x)$  prior was applied to the data but to reduce over-parameterisation  
258 we adopted a strict clock and the HKY substitution model (Hasegawa *et al.*, 1985) to locus-  
259 specific partitions following the EBSP tutorial (<http://www.beast2.org/tutorials>). Chain length  
260 ranged from 50 to 300 million generations, sampling every 10,000 generations. Convergence,  
261 population size changes, and ESS values were assessed using TRACER, ESPB plots were  
262 visualised using R (R CORE TEAM, 2017).

263 Finally, to investigate patterns suggestive of isolation by distance across all multi-  
264 distributed sooglossid taxa, we performed Mantel tests with 999 permutations on  
265 independent (to reduce conflict from incomplete sampling) *16s* and *cytb* matrices using the  
266 VEGAN package (Oksanen *et al.*, 2017) in R (R CORE TEAM, 2017). The GEOGRAPHIC DISTANCE  
267 MATRIX GENERATOR v. 1.2.3 (Ersts, 2012) was used to generate pairwise distance matrices  
268 for geographic localities. Sequences without corresponding geographic data were omitted.  
269 Sampling localities are shown in Fig. 1.

270

## 271 RESULTS

### 272 Molecular phylogeny and genetic variation

273 Our final mtDNA sequence alignment of 56 sooglossids (*So. thomasseti* = 9, *So sechellensis* =

274 37, *Se. gardineri* = 9, *Se. pipilodryas* = 1) contained corresponding sequence data totalling  
275 1,080 sites for 51 individuals. We were unable to obtain *cytb* sequence data for five Silhouette  
276 *Se. gardineri*, which constituted the majority (82%) of the total missing data of 3%. Rather  
277 than omit Silhouette *Se. gardineri* from our analyses (we are unaware of alternative *cytb* data  
278 for this taxon) we chose to maintain taxonomic coverage in all tree reconstructions.

279 Indels were present in the *16s* (*So. thomasseti* x1 double bp; *Se. gardineri* x2 single bp;  
280 *Se pipilodryas* x3 single bp) and *pomc* (*Sechellophryne* spp. x1 triple bp) sequence profiles. No  
281 evidence of saturation, or recombination events was detected in coding loci. Summary  
282 statistics of informative, uninformative, variable, and constant sites are shown in Table 1.  
283 Uncorrected and corrected genetic distances between taxa show values of 5.8%-14.0% and  
284 6.1%-15.6% respectively (Table 2). Between population genetic distances are 2.0%-4.5%  
285 (uncorrected) and 2.1%-4.7% (corrected) for *So. sechellensis*; 2.1% for *So. thomasseti*  
286 (uncorrected and corrected); and 3.6% (uncorrected) and 3.7% (corrected) for *Se. gardineri*  
287 (Table 3).

288 Our Bayesian and maximum likelihood mtDNA reconstructions displayed highly  
289 concordant internal topologies (Fig. 2; Fig. S1.1), and recovered full support for the  
290 monophyly of *Sooglossus* and *Sechellophryne*. Island-specific populations of *Se. gardineri* and  
291 *So. thomasseti* are strongly supported. Geographic structuring in *So. sechellensis* receives  
292 strong support in BI analysis but moderate support in the ML tree, recovering a sister  
293 relationship between Mahé frogs and a clade comprising those from Silhouette and Praslin.  
294 A further distinction between Silhouette and Praslin populations receives strong support.  
295 Bayesian phylogenetic reconstructions applying the Yule tree prior reflect that of analyses  
296 using the constant population tree prior but provide reduced support for the monophyly of  
297 *Sooglossus* and independent island populations of *Se. gardineri* and *So. Sechellensis* (Fig.

298 S1.2).

299

### 300 **Species trees and population boundaries**

301 The multilocus species trees are broadly congruent with our mtDNA phylogenies (Fig. 2-3).

302 The single topological disparity being internal relationships of *So. sechellensis* whereby the

303 nuDNA species tree places Praslin frogs as sister to a clade comprised of those from Mahé

304 and Silhouette. This contrasts with the mtDNA phylogeny and species trees which place Mahé

305 frogs as sister to a Praslin and Silhouette clade. Clades and sub-clades are generally well

306 supported except in the nuDNA tree where *Sooglossus* and *Sechellophryne* receive moderate

307 support, and the sister taxon relationship between the Mahé and Silhouette populations of

308 *Se. gardineri* is unresolved.

309 Ten well-supported entities are indicated from bPTP analyses, eight of which

310 correspond with island populations of the multi-distributed sooglossid taxa shown in the

311 mtDNA phylogeny (Fig. 2; Table S1.5). The remaining two entities represent members of an

312 internal clade of *So. sechellensis* on Mahé; one a single sample from the southern-most

313 population, the other comprised of one sample from the southern-most population and one

314 from a more northerly locality (Fig. 1-2; Fig. S1.1-2; Table S1.5).

315

### 316 **Nuclear DNA haplotypes**

317 For each of the four nuclear loci, constructed networks show two or more high-frequency

318 haplotypes in combination with multiple species- and population-specific haplotypes (Fig. 4-

319 7). In the network for *pomc* (36 haplotypes; Fig. 4) two mutational steps separated both *So.*

320 *sechellensis* and *So. thomasseti*, and the Mahé and Silhouette populations of *Se. gardineri*.

321 One haplotype was shared between genera for *rag1* (37 haplotypes; Fig. 5) with seven

322 mutational steps separating *So. sechellensis* and *So. thomasseti*. The *rag2* network (123  
323 haplotypes; Fig. 6) shows five mutational steps separating *So. sechellensis* and *So. thomasseti*,  
324 and two mutational steps between one of the two *Se. pipilodryas* haplotypes and *Se.*  
325 *gardineri*. No genus specific characters were observed for *rho* (26 haplotypes; Fig. 7) where  
326 four haplotypes were shared between *Sooglossus* and *Sechellophryne*. Given the analytical  
327 thresholds we set, three networks (*pomc*, *rag1*, *rag2*) were divergent enough to differentiate  
328 (disconnect) genera and identify independent haplotypes for *Se. pipilodryas*. All loci displayed  
329 unique island-specific haplotypes for each multi-distributed species.

330

### 331 **Population demography**

332 Neutrality tests to understand population demographics in the Sooglossidae showed mostly  
333 negative values, indicating positive selection or recent population expansion (Table S1.6).  
334 However, statistically significant negative values are observed only in calculations of  $F_S$ , which  
335 may be less effective with small sample sizes (Ramos-Onsins & Rozas, 2002). Statistically  
336 significant positive values are evident in *16s* for all three species for Tajima's  $D$  but not  $F_S$ .  
337 Tajima's  $D$  is not as powerful as either  $F_S$  or the  $R_2$  test statistic, and the  $R_2$  test is considered  
338 to be more effective when applied to smaller sample sizes (Ramos-Onsins & Rozas, 2002;  
339 Ramirez-Soriano *et al.*, 2008). Significant positive values ( $P < 0.05$ ) for a single locus in each  
340 species (*cytb*: *Se. gardineri*; *rag2*: *So. sechellensis*; *pomc*: *So. thomasseti*) were returned for  
341 the  $R_2$  test. This suggests a lack of congruence that may be more indicative of differential  
342 levels of ancestral polymorphisms, selective pressures, and substitution rates across species  
343 and among loci, than statistically significant departures from neutrality.

344 In EBSM analyses the 95% highest posterior density (HPD) interval returned for Mahé  
345 and Silhouette populations of *So. sechellensis*, *So. thomasseti* and *Se. gardineri* included 0,

346 therefore a constant population size for these taxa cannot be rejected (Table S1.7; Fig. S1.3-  
347 5). However, recent (within the last ~20 k years) population expansion appears to have  
348 occurred in *So. sechellensis* on Praslin (Fig. S1.3).

349

### 350 **Isolation by distance**

351 Matrices for our investigation of the effect of isolation by distance comprised 149 *So.*  
352 *sechellensis*, 29 *So. thomasseti*, and 26 *Se. gardineri* for *16s*, and 39 *So. sechellensis* and 9 *So.*  
353 *thomasseti* for *cytb*. Mantel tests indicated significant correlation between genetic and  
354 geographic distances in all species for both loci (*16s*: *So. sechellensis*,  $r = 0.8253$ ,  $P < 0.001$ ;  
355 *So. thomasseti*,  $r = 0.9895$ ,  $P < 0.001$ ; *Se. gardineri*,  $r = 0.9642$ ,  $P < 0.001$ ; *cytb*: *So. sechellensis*,  
356  $r = 0.6995$ ,  $P < 0.001$ ; *So. thomasseti*,  $r = 0.9755$ ,  $P < 0.05$ ).

357

## 358 **DISCUSSION**

### 359 **Sooglossid phylogeny and genetic differentiation**

360 Our analyses provide the first multi-gene phylogeny to use island-specific sampling to reveal  
361 intraspecific relationships within this endemic family. The mtDNA phylogeny supports our first  
362 hypothesis—that cryptic sooglossid diversity exists across the three islands where these frogs  
363 occur—and confirms the evolutionary distinctiveness of multiple geographically restricted  
364 sooglossid populations (Fig. 2). Our second hypothesis—that cryptic diversity corresponds  
365 with biogeographic (island) origin—is supported by independent evolutionary histories for  
366 the multi-distributed *Sooglossus* and *Sechellophryne* spp. in the mtDNA phylogeny, with  
367 distinct populations of *So. sechellensis* on Mahé, Silhouette, and Praslin, and *So. thomasseti*  
368 and *Se. gardineri* on Mahé and Silhouette (Fig. 2).

369 Mean uncorrected genetic distances among taxa for *16s* clearly reflect the greater



370 differences expected between genera (range: 12.32%-14.04%; Table 2). Within genera, the  
371 Jukes-Cantor (JC) corrected  $p$ -distances between *So. sechellensis* and *So. thomasseti* (6.1%),  
372 and *Se. gardineri* and *Se. pipilodryas* (7.0%) exceed the values previously reported by van der  
373 Meijden *et al.* (2007) (4.4% in *Sooglossus* and 5.7% in *Sechellophryne*) for sequence data of  
374 comparable length. However, van der Meijden *et al.* (2007) sampled considerably fewer than  
375 20 individuals in each case (*Sooglossus*:  $n = 7$ ; *Sechellophryne*:  $n = 2$ ); a limitation associated  
376 with an increased probability of underestimation of nucleotide diversity (Luo *et al.*, 2015).  
377 Estimations of genetic distance resulting from increased sampling are therefore more likely  
378 to represent the true population mean (Luo *et al.*, 2015).

379         van der Meijden *et al.* (2007) also identified a JC corrected  $p$ -distance of 3.0% between  
380 the Mahé and Silhouette populations of *So. thomasseti* but did so from four samples; two  
381 from Mahé, two from Silhouette. We report a JC corrected  $p$ -distance of 2.1% from a pool of  
382 29 individuals (Table 3) originating from four sites on the island of Mahé, and two sites on  
383 Silhouette. The spatial representation of our sampling, and greater sample size is therefore  
384 more likely to reflect a value closer to the true mean. Taylor *et al.* (2012) found uncorrected  
385 *16s*  $p$ -distances of 4.1%-6.1% between the Mahé, Silhouette, and Praslin populations of *So.*  
386 *sechellensis* from a total sample size of 26. We incorporate all but two of the *16s* sequences  
387 arising from Taylor *et al.* (2012) (these two omissions are Praslin samples placed within the  
388 Mahé clade in their study which are likely to be the result of laboratory contamination, as  
389 subsequent *cytb* analysis reflects their geographic origin; J. Labisko, unpubl. data) and report  
390 genetic distances of 2.1%-4.7% from 159 samples (Table 3).

391

### 392 **Species trees and population boundaries**

393 The multilocus species trees are highly congruent with our mtDNA phylogenies but clade

394 support differs between the mtDNA and nuDNA analyses (Fig. 3). The lower levels of support  
395 displayed may reflect statistical inaccuracy from missing (*cytb*) sequence data as well as the  
396 inherent differential qualities of the loci we sampled. While the specific status of *Sooglossus*  
397 and *Sechellophryne* taxa are not in question, further exploration of the data incorporating  
398 additional loci may elucidate the strength of relationship between the two isolated  
399 populations of *Se. gardineri*. Overall, and in spite of topological disparity between two island  
400 lineages of *So. sechellensis*, the multispecies coalescent and bPTP model independently  
401 provide further support for the monophyly of multiple island-specific lineages of sooglossid  
402 frogs. For *So. sechellensis*, bPTP results also indicate additional intraspecific structure within  
403 the Mahé population.

404

#### 405 **Nuclear variation**

406 There is an increasing body of evidence reporting discordant patterns between mtDNA and  
407 nuDNA markers in animal systems (Toews & Brelsford, 2012). Discordance between  
408 molecular markers may be especially pronounced in amphibians (Hoelzer, 1997; Monsen &  
409 Blouin, 2003), and nuclear genes are frequently recognised for their conflicting results in  
410 genealogical estimations in amphibian studies (e.g. Fisher-Reid & Wiens, 2011; Eto & Matsui,  
411 2014). Our analyses identified multiple haplotypes shared between island populations,  
412 species, and genera. Nevertheless, geographic structuring of the Sooglossidae is visibly  
413 evident in the nuclear loci we sampled, showing numerous unique haplotypes across all multi-  
414 distributed taxa and a commonality between our mtDNA and nuDNA datasets. While these  
415 nuDNA patterns may indicate a level of diversity within each population that differentiates it  
416 from congeners on other islands, the data are also likely to reflect incomplete sampling and  
417 incomplete lineage sorting; the latter especially so considering maternal line of inheritance

418 and smaller effective population size of mtDNA in comparison to the diploid, bi-parental  
419 nature of nuDNA.

420

#### 421 **Biogeographic and conservation implications**

422 Due to their intolerance of salt water, trans-oceanic dispersal is assumed to be an infrequent  
423 method of range expansion for amphibians (Duellman & Trueb, 1986; Green *et al.*, 1988; de  
424 Queiroz, 2005). The presence of endemic amphibians on oceanic islands may therefore be  
425 considered unusual, yet rafting is increasingly cited as an explanation for transoceanic  
426 dispersal of frogs (Vences *et al.*, 2003; Heinicke *et al.*, 2007; Maddock *et al.*, 2014; Bell *et al.*,  
427 2015a; Bell *et al.*, 2015b), and even caecilians (Measey *et al.*, 2006). However, in each case,  
428 pioneering dispersers have mainland congeners. Aside from their sister taxon relationship  
429 with the Nasikabatrachidae of India's Western Ghats, from which they may have diverged 66-  
430 131 Ma—prior to the geographic separation of India and Seychelles (Biju & Bossuyt, 2003;  
431 Roelants *et al.*, 2007; Ruane *et al.*, 2011; Pyron, 2014; Frazão *et al.*, 2015; Feng *et al.*, 2017)—  
432 the Sooglossidae have no recent relatives. The level of evolutionary distinctiveness displayed  
433 by these frogs, undoubtedly a result of their lengthy isolation, is clearly evidence of their  
434 historic and continuing presence on the archipelago.

435         Following its separation from India, the inner Seychelles region has formed both a  
436 continuous landmass of some 129,500 km<sup>2</sup>, and been submerged to its present extent,  
437 comprising an archipelago of 45 inner-islands covering ~247 km<sup>2</sup>. Had the Seychelles Bank  
438 ever been completely submerged, this would be strongly reflected in the composition of its  
439 fauna and flora, with an expectation of greater similarity to that of Africa and/or Asia  
440 (Nussbaum, 1984). The region has been subject to eustatic fluctuations, climatic variability,  
441 and vicariant events, which have played an influential role in the distribution of its biota.

442 Recently identified phylogeographic patterns within the archipelago's endemic herpetofauna  
443 have revealed a variety of geographic correlations: skinks and geckos broadly differentiate  
444 into northern (Praslin and surrounding islands) and southern (Mahé, Silhouette, and  
445 surrounding islands) groups (Rocha *et al.*, 2010; Rocha *et al.*, 2011; Rocha *et al.*, 2013; Valente  
446 *et al.*, 2013; Rocha *et al.*, 2016a; Rocha *et al.*, 2016b); while for the non-sooglossid anurans, a  
447 distinct lack of variability is shown in the multi-distributed treefrog *Tachycnemis seychellensis*  
448 (Maddock *et al.*, 2014), conflicting with observed structuring in Seychelles endemic caecilians  
449 (Adamson *et al.*, 2016; Maddock *et al.*, 2016; Maddock *et al.*, 2017). Our mtDNA analyses  
450 appear to confirm the relationship posited by Taylor *et al.* (2012), namely that Silhouette and  
451 Praslin populations of *So. sechellensis* comprise a clade sister to that of frogs from Mahé. Yet  
452 our nuDNA species tree presents a topological contrast by inferring Praslin frogs as sister to a  
453 Silhouette and Mahé clade; harmonious with the north-south split identified in other  
454 Seychelles herpetofauna. This disparity raises the question as to what these conflicting  
455 biogeographic patterns in the data may reflect.

456         Since the Late Pleistocene, regional instability caused by either hydro-isostatic uplift  
457 of the Seychelles Bank or volcanic subsidence (Montaggioni & Hoang, 1988) and substantial  
458 low sea-level stands (Colonna *et al.*, 1996; Camoin *et al.*, 2004) have likely generated irregular  
459 cycles of biogeographic isolation and reconnection across the Seychelles. Bathymetric data  
460 indicate a sea-level drop of ~60 m bpsl would effectively link the granitic islands (Rocha *et al.*,  
461 2013; Ali, 2018), providing the opportunity for dispersal and connection/reconnection of  
462 previously disparate populations. Incongruence between and among the phylogeographic  
463 patterns exhibited by Seychelles' herpetofauna are undoubtedly the result of a number of  
464 contributory factors, including the inherent ecology and dispersal ability of each taxon.  
465 Although these and other aspects are yet to be fully explored, Maddock *et al.* (2014) found

466 low levels of genetic variation in *T. seychellensis* concluding, *inter-alia*, that relatively recent  
467 admixture during low sea-level stands may explain this observation. The treefrogs are  
468 regularly encountered in appropriate habitat at lower elevations down to sea-level, and may  
469 on occasion raft across the ocean as a means of dispersal, as their ancestors are believed to  
470 have done from Madagascar (Vences *et al.*, 2003; Maddock *et al.*, 2014). The terrestrial  
471 Sooglossidae (although *Sechellophryne* spp. may be observed in low-level vegetation; Gerlach  
472 & Willi, 2002; J. Labisko, pers. obs.) are generally restricted to high elevation moist forest,  
473 such that lower (and dryer) elevations combined with even a limited oceanic distance  
474 between suitable habitats, may act as a considerable barrier to dispersal. However, the  
475 islands of Mahé and Silhouette share high elevation peaks, similar forest habitat, and are  
476 currently separated by less than 20 km, and given a significant drop in sea level, the  
477 opportunity for dispersal between the two would inevitably increase. Mahé and Silhouette  
478 frogs may therefore be expected to share greater similarities than either do with those from  
479 Praslin—an island which is lower, drier, 37 km distant from Mahé, and 51 km from  
480 Silhouette—and the locus-specific nuDNA gene trees produced in our multispecies coalescent  
481 analyses display a largely congruent topology, suggesting these loci are representative of true  
482 relationships across the nuclear genome.

483         Clear geographic patterns of discordance between mtDNA and nuDNA are likely to  
484 exclude incomplete lineage sorting as an underlying explanation, and may instead indicate  
485 biogeographic discordance (Funk & Omland, 2003; Toews & Brelsford, 2012). Extended  
486 periods of isolation combined with previous range contact are an intrinsic factor in most taxa  
487 that display patterns of this nature, during which high frequency mutations accumulate and  
488 are followed by interbreeding in hybrid zones upon range reconnection, generating divergent  
489 patterns in the mtDNA and nuDNA genomes (Toews & Brelsford, 2012). The cycles of

490 emergence and submergence of the Seychelles Bank are unknown but the patterns of genetic  
491 differentiation and population demography we report could be attributed to infrequent  
492 stable environmental conditions of adequate duration that would arise as a result of  
493 significant but sporadic eustatic fluctuations, and should not be discounted as a mechanism  
494 to explain the patterns observed in our data. It is noteworthy that one population—*So.*  
495 *sechellensis* from Praslin—appears to have recently expanded (Fig. S1.3). That no other  
496 sooglossids are found on Praslin suggests that (i) *So. sechellensis* is the only sooglossid to have  
497 occurred here, or (ii) other members of the Sooglossidae have since died out, perhaps as a  
498 result of the climactic effects and loss of terrestrial habitat following deglaciation and the rise  
499 in sea levels from the Late Pleistocene to Early Holocene (Dutton *et al.*, 2015; Woodroffe *et*  
500 *al.*, 2015). In either scenario, the Praslin frogs have seemingly been successful in exploiting  
501 available habitat on this island in the absence of other sooglossids.

502         Reciprocal monophyly in mtDNA together with significant divergence in nuDNA loci  
503 have long been criteria for defining evolutionarily significant units (Moritz, 1994). Our results  
504 meet these criteria, showing numerous unique, geographically specific haplotypes in nuclear  
505 loci, and reciprocal monophyly in mtDNA for sooglossid populations, additional analyses of  
506 which indicates significant effects of isolation by distance. Sooglossid lineages that reflect  
507 island origin are defined across all multi-distributed species: *So. sechellensis* on Mahé,  
508 Silhouette, and Praslin, and *So. thomasseti* and *Se. gardineri* on Mahé and Silhouette (Fig. 2-  
509 3). Furthermore, and in accordance with the criteria ascribed by Vieites *et al.* (2009), we  
510 consider these lineages as unconfirmed candidate species. Given the limitations of species  
511 delimitation methods in distinguishing structure from population isolation versus species  
512 boundaries (Sukumaran & Knowles, 2017; Leaché *et al.*, 2018) (evidenced in our study by the  
513 identification of intraspecific structure within the Mahé population of *So. sechellensis*; Fig. 2;

514 Table S1.5), a continuing formal taxonomic appraisal for the Sooglossidae, combining multiple  
515 lines of evidence to corroborate hypotheses of distinct lineages is underway and will be  
516 presented elsewhere.

517 Our investigation of an understudied insular taxon, endemic to the Seychelles  
518 archipelago, adds to the developing biogeographic picture of this unique region. Patterns of  
519 cryptic diversity in Seychelles' amphibians have only recently begun to be explored, yet  
520 already appear to be highly prevalent and complex. Prior to our study, four sooglossid species  
521 were recognised across the three islands upon which they occur, with one population—the  
522 only sooglossid found on the island of Praslin, *So. sechellensis*—determined as fitting the  
523 criteria of an additional ESU (Taylor *et al.*, 2012). The cryptic diversity we have uncovered  
524 denotes a total of eight independent island lineages that should be managed accordingly.  
525 Such management action should include regular long-term population and habitat  
526 assessments, support of the genetic integrity of each ESU by carrying out no inter-island  
527 translocations, and the establishment of regular screening activities for invasive pathogens  
528 including *Batrachochytrium dendrobatidis*, *B. salamandrivorans*, and *Ranavirus*—notably, the  
529 Seychelles is one of only two global regions where pathogenic chytrid is yet to be detected  
530 (Labisko *et al.*, 2015; Lips, 2016). The identification of distinct, island-specific populations of  
531 these frogs warrants continued investigation of their intraspecific relationships, and further  
532 insights are likely to reveal additional factors important for their future conservation.

533

#### 534 **ACKNOWLEDGEMENTS**

535 We express our gratitude for support provided by the Darwin Initiative (grant 19-002 to RAG  
536 and JJG); Durrell Institute of Conservation and Ecology; The Natural History Museum, London;  
537 Seychelles Islands Foundation; Seychelles National Parks Authority; The Systematics

538 Association and The Linnean Society (independent Systematics Research Fund awards to JL  
539 and STM); University College London; and the University of Kent. We thank the Seychelles  
540 Bureau of Standards for permission to carry out fieldwork; Seychelles Department of  
541 Environment for permission to collect and export samples; Matthieu La Buschagne for access  
542 to Coco de Mer Hotel land on Praslin; Island Conservation Society for field assistance on  
543 Silhouette; Islands Development Company for permission and hosting on Silhouette; and  
544 Rachel Bristol for organisational and field assistance. We also thank The Mohammad bin  
545 Zayed Species Conservation Fund for their continuing support of JL (Project 172515128) and  
546 STM (Project 162513749). Wilna Accouche, Katy Beaver, Darryl Birch, Georgia French, David  
547 Gower, Philip Haupt, Marc Jean-Baptiste, Christopher Kaiser-Bunbury, Pete Haverson, James  
548 Mougat, Marcus Pierre, Nathachia Pierre, Dainise Quatre, Anna Reuleaux, Heather Richards,  
549 Mark Wilkinson, and many other NGO staff, researchers, and Seychellois provided in- and ex-  
550 situ support, for which we are especially grateful. We thank Katy Beaver, Jeff Streicher, Ben  
551 Tapley, and three anonymous reviewers for helpful comments on previous drafts of this  
552 manuscript.



## 553 REFERENCES

- 554 **Adamson EAS, Saha A, Maddock ST, Nussbaum RA, Gower DJ, Streicher JW. 2016.**  
555       Microsatellite discovery in an insular amphibian (*Grandisonia alternans*) with  
556       comments on cross-species utility and the accuracy of locus identification from  
557       unassembled Illumina data. *Conservation Genetics Resources* **8**: 541-551.
- 558 **Adersen H. 1995.** Research on islands: Classic, recent, and prospective approaches. In:  
559       Vitousek PM, Loope LL and Adersen H, eds. *Islands*. Berlin, Heidelberg: Springer Berlin  
560       Heidelberg. 7-21.
- 561 **Ali JR. 2017.** Islands as biological substrates: classification of the biological assemblage  
562       components and the physical island types. *Journal of Biogeography* **44**: 984-994.
- 563 **Ali JR. 2018.** Islands as biological substrates: Continental. *Journal of Biogeography* **45**: 1003-  
564       1018.
- 565 **Alonso R, Crawford AJ, Bermingham E. 2012.** Molecular phylogeny of an endemic radiation  
566       of Cuban toads (Bufonidae: *Peltophryne*) based on mitochondrial and nuclear genes.  
567       *Journal of Biogeography* **39**: 434-451.
- 568 **Bell RC, Drewes RC, Channing A, Gvoždík V, Kielgast J, Lötters S, Stuart BL, Zamudio KR,**  
569       **Emerson B. 2015a.** Overseas dispersal of *Hyperolius* reed frogs from Central Africa to  
570       the oceanic islands of São Tomé and Príncipe. *Journal of Biogeography* **42**: 65-75.
- 571 **Bell RC, Drewes RC, Zamudio KR. 2015b.** Reed frog diversification in the Gulf of Guinea:  
572       overseas dispersal, the progression rule, and in situ speciation. *Evolution* **69**: 904-915.
- 573 **Biju SD, Bossuyt F. 2003.** New frog family from India reveals an ancient biogeographical link  
574       with the Seychelles. *Nature* **425**: 711-714.
- 575 **Boettger O. 1896.** Neue Kriechthiere (Scelotes, *Arthroleptis*) von den Seychellen. *Zoologischer*  
576       *Anzeiger* **19**: 349.

- 577 **Bouckaert R, Heled J, Kuhnert D, Vaughan T, Wu CH, Xie D, Suchard MA, Rambaut A,**  
578 **Drummond AJ. 2014.** BEAST 2: a software platform for Bayesian evolutionary analysis.  
579 *PLoS Computational Biology* **10**: e1003537.
- 580 **Boulenger GA. 1909.** No. XVI.-A list of the freshwater fishes, batrachians, and reptiles  
581 obtained by Mr. J. Stanley Gardiner's expedition to the Indian Ocean. *Transactions of*  
582 *the Linnean Society of London. 2nd Series: Zoology* **12**: 291-300.
- 583 **Boulenger GA. 1911.** No. XVII.-List of the batrachians and reptiles obtained by Prof. Stanley  
584 Gardiner on his second expedition to the Seychelles and Aldabra. *Transactions of the*  
585 *Linnean Society of London. 2nd Series: Zoology* **14**: 375-378.
- 586 **Camoin GF, Montaggioni LF, Braithwaite CJR. 2004.** Late glacial to post glacial sea levels in  
587 the western Indian Ocean. *Marine Geology* **206**: 119-146.
- 588 **Castresana J. 2000.** Selection of conserved blocks from multiple alignments for their use in  
589 phylogenetic analysis. *Molecular Biology and Evolution* **17**: 540-552.
- 590 **Chatterjee S, Goswami A, Scotese CR. 2013.** The longest voyage: Tectonic, magmatic, and  
591 paleoclimatic evolution of the Indian plate during its northward flight from Gondwana  
592 to Asia. *Gondwana Research* **23**: 238-267.
- 593 **Clement M, Posada D, Crandall KA. 2000.** TCS: a computer program to estimate gene  
594 genealogies. *Molecular Ecology* **9**: 1657-1659.
- 595 **Collier JS, Sansom V, Ishizuka O, Taylor RN, Minshull TA, Whitmarsh RB. 2008.** Age of  
596 Seychelles–India break-up. *Earth and Planetary Science Letters* **272**: 264-277.
- 597 **Colonna M, Casanova J, Dullo W-C, Camoin G. 1996.** Sea-level changes and  $\delta^{18}\text{O}$  record for  
598 the past 34,000 yr from Mayotte Reef, Indian Ocean. *Quaternary Research* **46**: 335-  
599 339.
- 600 **Cronk QCB. 1997.** Islands: stability, diversity, conservation. *Biodiversity and Conservation* **6**:

- 601 477-493.
- 602 **Darwin C. 1859.** *On the origin of species*. Murray: London.
- 603 **Davies D, Francis TJG. 1964.** The crustal structure of the Seychelles bank. *Deep Sea Research*  
604 *and Oceanographic Abstracts* **11**: 921-927.
- 605 **de Queiroz A. 2005.** The resurrection of oceanic dispersal in historical biogeography. *Trends*  
606 *in Ecology and Evolution* **20**: 68-73.
- 607 **Delpont W, Poon AF, Frost SD, Kosakovsky Pond SL. 2010.** Datamonkey 2010: a suite of  
608 phylogenetic analysis tools for evolutionary biology. *Bioinformatics* **26**: 2455-2457.
- 609 **Drummond AJ, Ho SY, Phillips MJ, Rambaut A. 2006.** Relaxed phylogenetics and dating with  
610 confidence. *PLoS Biology* **4**: e88.
- 611 **Drummond AJ, Rambaut A. 2007.** BEAST: Bayesian evolutionary analysis by sampling trees.  
612 *BMC Evolutionary Biology* **7**: 214.
- 613 **Duellman WE, Trueb L. 1986.** *Biology of amphibians*. Johns Hopkins University Press.
- 614 **Dutton A, Webster JM, Zwartz D, Lambeck K, Wohlfarth B. 2015.** Tropical tales of polar ice:  
615 evidence of Last Interglacial polar ice sheet retreat recorded by fossil reefs of the  
616 granitic Seychelles islands. *Quaternary Science Reviews* **107**: 182-196.
- 617 **Dyer M, Sailsbery J, McClellan D. n.d.** DataConvert—biological data file conversion. Available  
618 at [http://www.mybiosoftware.com/dataconvert-1-0-converts-proteindna-data-](http://www.mybiosoftware.com/dataconvert-1-0-converts-proteindna-data-formats.html)  
619 [formats.html](http://www.mybiosoftware.com/dataconvert-1-0-converts-proteindna-data-formats.html)
- 620 **Edgar RC. 2004.** MUSCLE: multiple sequence alignment with high accuracy and high  
621 throughput. *Nucleic Acids Research* **32**: 1792-1797.
- 622 **Ersts P. 2012.** Geographic Distance Matrix Generator version 1.23: American Museum of  
623 Natural History.
- 624 **Eto K, Matsui M. 2014.** Cytonuclear discordance and historical demography of two brown

- 625 frogs, *Rana tagoi* and *R. sakuraii* (Amphibia: Ranidae). *Molecular Phylogenetics and*  
626 *Evolution* **79**: 231-239.
- 627 **Felsenstein J. 1981.** Evolutionary trees from DNA sequences: a maximum likelihood approach.  
628 *Journal of Molecular Evolution* **17**: 368-376.
- 629 **Feng YJ, Blackburn DC, Liang D, Hillis DM, Wake DB, Cannatella DC, Zhang P. 2017.**  
630 Phylogenomics reveals rapid, simultaneous diversification of three major clades of  
631 Gondwanan frogs at the Cretaceous-Paleogene boundary. *Proceedings of the National*  
632 *Academy of Sciences of the United States of America* **114**: E5864-E5870.
- 633 **Fisher-Reid MC, Wiens J. 2011.** What are the consequences of combining nuclear and  
634 mitochondrial data for phylogenetic analysis? Lessons from *Plethodon* salamanders  
635 and 13 other vertebrate clades. *BMC Evolutionary Biology* **11**: 300.
- 636 **Frazão A, da Silva HR, Russo CA. 2015.** The Gondwana breakup and the history of the Atlantic  
637 and Indian Oceans unveils two new clades for early neobatrachian diversification. *PLoS*  
638 *One* **10**: e0143926.
- 639 **Frost DR, Grant T, Faivovich J, Bain RH, Haas A, Haddad CFB, De Sá RO, Channing A,**  
640 **Wilkinson M, Donnellan SC, Raxworthy CJ, Campbell JA, Blotto BL, Moler P, Drewes**  
641 **RC, Nussbaum RA, Lynch JD, Green DM, Wheeler WC. 2006.** The Amphibian Tree of  
642 Life. *Bulletin of the American Museum of Natural History* **297**: 1-291.
- 643 **Fu YX. 1997.** Statistical tests of neutrality of mutations against population growth, hitchhiking  
644 and background selection. *Genetics* **147**: 915-925.
- 645 **Funk DJ, Omland KE. 2003.** Species-level paraphyly and polyphyly: Frequency, causes, and  
646 consequences, with insights from animal mitochondrial DNA. *Annual Review of*  
647 *Ecology, Evolution, and Systematics* **34**: 397-423.
- 648 **Gene Codes Corporation. 2015.** Sequencher® version 5.3 sequence analysis software. Ann

- 649 Arbor, MI USA.
- 650 **Gerlach J, Willi J. 2002.** A new species of frog, genus *Sooglossus* (Anura, Sooglossidae) from  
651 Silhouette Island, Seychelles. *Amphibia-Reptilia* **23**: 445-458.
- 652 **Gissi C, San Mauro D, Pesole G, Zardoya R. 2006.** Mitochondrial phylogeny of Anura  
653 (Amphibia): a case study of congruent phylogenetic reconstruction using amino acid  
654 and nucleotide characters. *Gene* **366**: 228-237.
- 655 **Glez-Pena D, Gomez-Blanco D, Reboiro-Jato M, Fdez-Riverola F, Posada D. 2010.** ALTER:  
656 program-oriented conversion of DNA and protein alignments. *Nucleic Acids Research*  
657 **38**: W14-18.
- 658 **Green DM, Nussbaum RA, Datong Y. 1988.** Genetic divergence and heterozygosity among  
659 frogs of the family Sooglossidae. *Herpetologica* **44**: 113-119.
- 660 **Haahr M. 2015.** True Random Number Service: <http://www.random.org>.
- 661 **Harrigan RJ, Mazza ME, Sorenson MD. 2008.** Computation vs. cloning: evaluation of two  
662 methods for haplotype determination. *Molecular Ecology Resources* **8**: 1239-1248.
- 663 **Hasegawa M, Kishino H, Yano T. 1985.** Dating of the human-ape splitting by a molecular clock  
664 of mitochondrial DNA. *Journal of Molecular Evolution* **22**: 160-174.
- 665 **Heinicke MP, Duellman WE, Hedges SB. 2007.** Major Caribbean and Central American frog  
666 faunas originated by ancient oceanic dispersal. *Proceedings of the National Academy*  
667 *of Sciences of the United States of America* **104**: 10092-10097.
- 668 **Heled J, Drummond AJ. 2008.** Bayesian inference of population size history from multiple loci.  
669 *BMC Evolutionary Biology* **8**: 289.
- 670 **Heled J, Drummond AJ. 2010.** Bayesian inference of species trees from multilocus data.  
671 *Molecular Biology and Evolution* **27**: 570-580.
- 672 **Hoelzer GA. 1997.** Inferring phylogenies from mtDNA variation: mitochondrial-gene trees

- 673           versus nuclear-gene trees revisited. *Evolution* **51**: 622-626.
- 674 **Huelsenbeck JP, Ronquist F, Nielsen R, Bollback JP. 2001.** Bayesian inference of phylogeny  
675           and its impact on evolutionary biology. *Science* **294**: 2310-2314.
- 676 **Irisarri I, San Mauro D, Green DM, Zardoya R. 2010.** The complete mitochondrial genome of  
677           the relict frog *Leiopelma archeyi*: insights into the root of the frog Tree of Life.  
678           *Mitochondrial DNA* **21**: 173-182.
- 679 **Isaac NJ, Redding DW, Meredith HM, Safi K. 2012.** Phylogenetically-informed priorities for  
680           amphibian conservation. *PLoS One* **7**: e43912.
- 681 **IUCN SSC Amphibian Specialist Group. 2013a.** *Sechellophryne gardineri* *The IUCN Red List of*  
682           *Threatened Species 2013.*
- 683 **IUCN SSC Amphibian Specialist Group. 2013b.** *Sechellophryne pipilodryas* *The IUCN Red List*  
684           *of Threatened Species 2013.*
- 685 **IUCN SSC Amphibian Specialist Group. 2013c.** *Sooglossus sechellensis* *The IUCN Red List of*  
686           *Threatened Species 2013.*
- 687 **IUCN SSC Amphibian Specialist Group. 2013d.** *Sooglossus thomasseti* *The IUCN Red List of*  
688           *Threatened Species 2013.*
- 689 **Jockusch EL, Martínez-Solano I, Timpe EK. 2015.** The effects of inference method, population  
690           sampling, and gene sampling on species tree inferences: An empirical study in slender  
691           salamanders (Plethodontidae: Batrachoseps). *Systematic Biology* **64**: 66-83.
- 692 **Kosakovsky Pond SL, Posada D, Gravenor MB, Woelk CH, Frost SD. 2006a.** Automated  
693           phylogenetic detection of recombination using a genetic algorithm. *Molecular Biology*  
694           *and Evolution* **23**: 1891-1901.
- 695 **Kosakovsky Pond SL, Posada D, Gravenor MB, Woelk CH, Frost SD. 2006b.** GARD: a genetic  
696           algorithm for recombination detection. *Bioinformatics* **22**: 3096-3098.

- 697 **Labisko J, Maddock ST, Taylor ML, Chong-Seng L, Gower DJ, Wynne FJ, Wombwell E, Morel**  
698 **C, French GCA, Bunbury N, Bradfield KS. 2015.** Chytrid fungus (*Batrachochytrium*  
699 *dendrobatidis*) undetected in the two orders of Seychelles amphibians. *Herpetological*  
700 *Review* **46**: 41-45.
- 701 **Lambert SM, Reeder TW, Wiens JJ. 2015.** When do species-tree and concatenated estimates  
702 disagree? An empirical analysis with higher-level scincid lizard phylogeny. *Molecular*  
703 *Phylogenetics and Evolution* **82 Pt A**: 146-155.
- 704 **Lanfear R, Calcott B, Ho SY, Guindon S. 2012.** Partitionfinder: combined selection of  
705 partitioning schemes and substitution models for phylogenetic analyses. *Molecular*  
706 *Biology and Evolution* **29**: 1695-1701.
- 707 **Leaché AD, Zhu T, Rannala B, Yang Z. 2018.** The spectre of too many species. *Systematic*  
708 *Biology*.
- 709 **Lepage T, Bryant D, Philippe H, Lartillot N. 2007.** A general comparison of relaxed molecular  
710 clock models. *Molecular Biology and Evolution* **24**: 2669-2680.
- 711 **Librado P, Rozas J. 2009.** DnaSP v5: a software for comprehensive analysis of DNA  
712 polymorphism data. *Bioinformatics* **25**: 1451-1452.
- 713 **Lips KR. 2016.** Overview of chytrid emergence and impacts on amphibians. *Philosophical*  
714 *transactions of the Royal Society of London. Series B, Biological sciences* **371**.
- 715 **Los Alamos National Security LLC. 2005-2006.** Format Converter: U.S. Department of Energy's  
716 National Nuclear Security Administration:  
717 [https://www.hiv.lanl.gov/content/sequence/FORMAT\\_CONVERSION/form.html](https://www.hiv.lanl.gov/content/sequence/FORMAT_CONVERSION/form.html)
- 718 **Luo A, Lan H, Ling C, Zhang A, Shi L, Ho SY, Zhu C. 2015.** A simulation study of sample size for  
719 DNA barcoding. *Ecology and Evolution* **5**: 5869-5879.
- 720 **MacArthur RH, Wilson EO. 1967.** *Theory of island biogeography*. Princeton University Press:

721 Princeton.

722 **Maddock ST, Briscoe AG, Wilkinson M, Waeschenbach A, San Mauro D, Day JJ, Littlewood**  
723 **DT, Foster PG, Nussbaum RA, Gower DJ. 2016.** Next-generation mitogenomics: A  
724 comparison of approaches applied to caecilian amphibian phylogeny. *PLoS One* **11:**  
725 e0156757.

726 **Maddock ST, Day JJ, Nussbaum RA, Wilkinson M, Gower DJ. 2014.** Evolutionary origins and  
727 genetic variation of the Seychelles treefrog, *Tachycnemis seychellensis* (Dumeril and  
728 Bibron, 1841) (Amphibia: Anura: Hyperoliidae). *Molecular Phylogenetics and Evolution*  
729 **75:** 194-201.

730 **Maddock ST, Wilkinson M, Nussbaum RA, Gower DJ. 2017.** A new species of small and highly  
731 abbreviated caecilian (Gymnophiona: Indotyphlidae) from the Seychelles island of  
732 Praslin, and a recharacterization of *Hypogeophis brevis* Boulenger, 1911. *Zootaxa*  
733 **4329:** 301.

734 **Maia-Carvalho B, Goncalves H, Ferrand N, Martinez-Solano I. 2014.** Multilocus assessment  
735 of phylogenetic relationships in *Alytes* (Anura, Alytidae). *Molecular Phylogenetics and*  
736 *Evolution* **79:** 270-278.

737 **Matthews DH, Davies D. 1966.** Geophysical studies of the Seychelles Bank. *Philosophical*  
738 *Transactions of the Royal Society A: Mathematical, Physical and Engineering Sciences*  
739 **259:** 227-239.

740 **Measey GJ, Vences M, Drewes RC, Chiari Y, Melo M, Bourles B. 2006.** Freshwater paths  
741 across the ocean: molecular phylogeny of the frog *Ptychadena newtoni* gives insights  
742 into amphibian colonization of oceanic islands. *Journal of Biogeography* **34:** 7-20.

743 **Miller MA, Pfeiffer W, Schwartz T. 2010.** Proceedings of the Gateway Computing  
744 Environments Workshop (GCE) *Creating the CIPRES science gateway for inference of*



- 745            *large phylogenetic trees*: IEEE New Orleans. 1-8.
- 746    **Monsen KJ, Blouin MS. 2003.** Genetic structure in a montane ranid frog: restricted gene flow  
747            and nuclear-mitochondrial discordance. *Molecular Ecology* **12**: 3275-3286.
- 748    **Montaggioni LF, Hoang CT. 1988.** The last interglacial high sea level in the granitic Seychelles,  
749            Indian ocean. *Palaeogeography, Palaeoclimatology, Palaeoecology* **64**: 79-91.
- 750    **Moritz C. 1994.** Defining 'Evolutionarily Significant Units' for conservation. *Trends in Ecology*  
751            *and Evolution* **9**: 373-375.
- 752    **Murias dos Santos A, Cabezas MP, Tavares AI, Xavier R, Branco M. 2016.** tcsBU: a tool to  
753            extend TCS network layout and visualization. *Bioinformatics* **32**: 627-628.
- 754    **Noble GK. 1931.** *The biology of the Amphibia*. McGraw-Hill Book Company, Inc.: New York  
755            and London.
- 756    **Nussbaum RA. 1984.** Amphibians of the Seychelles. In: Stoddart DR, ed. *Biogeography and*  
757            *ecology of the Seychelles Islands*. The Hague; Boston: Hingham, Massachusetts, USA:  
758            W. Junk. 379-415.
- 759    **Oksanen J, Blanchet FG, Friendly M, Kindt R, Legendre P, McGlinn D, Minchin PR, O'Hara RB,**  
760            **Simpson GL, Solymos P, M. Henry H. Stevens, Szoecs E, Wagner H. 2017.** vegan:  
761            Community Ecology Package. 2.4-4. ed.
- 762    **Paulay G. 1994.** Biodiversity on oceanic Islands: Its origin and extinction. *American Zoologist*  
763            **34**: 134-144.
- 764    **Pond SL, Frost SD. 2005.** Datamonkey: rapid detection of selective pressure on individual sites  
765            of codon alignments. *Bioinformatics* **21**: 2531-2533.
- 766    **Pyron RA. 2014.** Biogeographic analysis reveals ancient continental vicariance and recent  
767            oceanic dispersal in amphibians. *Systematic Biology* **63**: 779-797.
- 768    **Pyron RA, Wiens JJ. 2011.** A large-scale phylogeny of Amphibia including over 2800 species,

- 769 and a revised classification of extant frogs, salamanders, and caecilians. *Molecular*  
770 *Phylogenetics and Evolution* **61**: 543-583.
- 771 **R Core Team. 2017.** R: A language and environment for statistical computing. Vienna, Austria.:  
772 R Foundation for Statistical Computing.
- 773 **Rambaut A. 2016.** FigTree 1.4.3.
- 774 **Rambaut A, Suchard MA, Xie D, Drummond AJ. 2014.** Tracer v1.6.
- 775 **Ramirez-Soriano A, Ramos-Onsins SE, Rozas J, Calafell F, Navarro A. 2008.** Statistical power  
776 analysis of neutrality tests under demographic expansions, contractions and  
777 bottlenecks with recombination. *Genetics* **179**: 555-567.
- 778 **Ramos-Onsins SE, Rozas J. 2002.** Statistical properties of new neutrality tests against  
779 population growth. *Molecular Biology and Evolution* **19**: 2092-2100.
- 780 **Robertson JM, Langin KM, Sillett TS, Morrison SA, Ghalambor CK, Funk WC. 2014.** Identifying  
781 evolutionarily significant units and prioritizing populations for management on  
782 islands. *Monographs of the Western North American Naturalist* **7**: 397-411.
- 783 **Rocha S, Harris D, Posada D. 2011.** Cryptic diversity within the endemic prehensile-tailed  
784 gecko *Urocotyledon inexpectata* across the Seychelles Islands: patterns of  
785 phylogeographical structure and isolation at the multilocus level. *Biological Journal of*  
786 *the Linnean Society* **104**: 177-191.
- 787 **Rocha S, Harris DJ, Carretero M. 2010.** Genetic diversity and phylogenetic relationships of  
788 *Mabuya* spp. (Squamata: Scincidae) from western Indian Ocean islands. *Amphibia-*  
789 *Reptilia* **31**: 375-385.
- 790 **Rocha S, Perera A, Bunbury N, Kaiser-Bunbury CN, Harris DJ. 2016a.** Speciation history and  
791 species-delimitation within the Seychelles Bronze geckos, *Ailuronyx* spp.: molecular  
792 and morphological evidence. *Biological Journal of the Linnean Society*.

- 793 **Rocha S, Perera A, Silva A, Posada D, Harris DJ. 2016b.** Evolutionary history of *Trachylepis*  
794 skinks in the Seychelles islands: introgressive hybridization, morphological evolution  
795 and geographic structure. *Biological Journal of the Linnean Society* **119**: 15-36.
- 796 **Rocha S, Posada D, Harris DJ. 2013.** Phylogeography and diversification history of the day-  
797 gecko genus *Phelsuma* in the Seychelles islands. *BMC Evolutionary Biology* **13**: 3.
- 798 **Roelants K, Gower DJ, Wilkinson M, Loader SP, Biju SD, Guillaume K, Moriau L, Bossuyt F.**  
799 **2007.** Global patterns of diversification in the history of modern amphibians.  
800 *Proceedings of the National Academy of Sciences of the United States of America* **104**:  
801 887-892.
- 802 **Ruane S, Pyron RA, Burbrink FT. 2011.** Phylogenetic relationships of the Cretaceous frog  
803 *Beelzebufo* from Madagascar and the placement of fossil constraints based on  
804 temporal and phylogenetic evidence. *Journal of Evolutionary Biology* **24**: 274-285.
- 805 **Salerno PE, Senaris JC, Rojas-Runjaic FJ, Cannatella DC. 2015.** Recent evolutionary history of  
806 Lost World endemics: population genetics, species delimitation, and phylogeography  
807 of sky-island treefrogs. *Molecular Phylogenetics and Evolution* **82 Pt A**: 314-323.
- 808 **Santos AMC, Field R, Ricklefs RE. 2016.** New directions in island biogeography. *Global Ecology*  
809 *and Biogeography* **25**: 751-768.
- 810 **Silvestro D, Michalak I. 2012.** raxmlGUI: a graphical front-end for RAxML. *Organisms Diversity*  
811 *& Evolution* **12**: 335-337.
- 812 **Stamatakis A. 2014.** RAxML version 8: a tool for phylogenetic analysis and post-analysis of  
813 large phylogenies. *Bioinformatics* **30**: 1312-1313.
- 814 **Stephens M, Donnelly P. 2003.** A comparison of bayesian methods for haplotype  
815 reconstruction from population genotype data. *American Journal of Human Genetics*  
816 **73**: 1162-1169.

- 817 **Stephens M, Scheet P. 2005.** Accounting for decay of linkage disequilibrium in haplotype  
818 inference and missing-data imputation. *American Journal of Human Genetics* **76**: 449-  
819 462.
- 820 **Stephens M, Smith NJ, Donnelly P. 2001.** A new statistical method for haplotype  
821 reconstruction from population data. *American Journal of Human Genetics* **68**: 978-  
822 989.
- 823 **Sukumaran J, Knowles LL. 2017.** Multispecies coalescent delimits structure, not species.  
824 *Proceedings of the National Academy of Sciences* **114**: 1607-1612.
- 825 **Tajima F. 1989.** Statistical method for testing the neutral mutation hypothesis by DNA  
826 polymorphism. *Genetics* **123**: 585-595.
- 827 **Talavera G, Castresana J. 2007.** Improvement of phylogenies after removing divergent and  
828 ambiguously aligned blocks from protein sequence alignments. *Systematic Biology* **56**:  
829 564-577.
- 830 **Tamura K, Stecher G, Peterson D, Filipowski A, Kumar S. 2013.** MEGA6: Molecular Evolutionary  
831 Genetics Analysis version 6.0. *Molecular Biology and Evolution* **30**: 2725-2729.
- 832 **Taylor ML, Bunbury N, Chong-Seng L, Doak N, Kundu S, Griffiths RA, Groombridge JJ. 2012.**  
833 Evidence for evolutionary distinctiveness of a newly discovered population of  
834 sooglossid frogs on Praslin Island, Seychelles. *Conservation Genetics* **13**: 557-566.
- 835 **Toews DP, Brelsford A. 2012.** The biogeography of mitochondrial and nuclear discordance in  
836 animals. *Molecular Ecology* **21**: 3907-3930.
- 837 **Vaidya G, Lohman DJ, Meier R. 2011.** SequenceMatrix: concatenation software for the fast  
838 assembly of multi-gene datasets with character set and codon information. *Cladistics*  
839 **27**: 171-180.
- 840 **Valente J, Rocha S, Harris DJ. 2013.** Differentiation within the endemic burrowing skink

- 841 *Pamelaescincus gardineri*, across the Seychelles islands, assessed by mitochondrial  
842 and nuclear markers. *African Journal of Herpetology* **63**: 25-33.
- 843 **van der Meijden A, Boistel R, Gerlach J, Ohler A, Vences M, Meyer A. 2007.** Molecular  
844 phylogenetic evidence for paraphyly of the genus *Sooglossus*, with the description of  
845 a new genus of Seychellean frogs. *Biological Journal of the Linnean Society* **91**: 347 -  
846 359.
- 847 **Vences M, Vieites DR, Glaw F, Brinkmann H, Kosuch J, Veith M, Meyer A. 2003.** Multiple  
848 overseas dispersal in amphibians. *Proceedings of the Royal Society B: Biological*  
849 *Sciences* **270**: 2435-2442.
- 850 **Vieites DR, Wollenberg KC, Andreone F, Kohler J, Glaw F, Vences M. 2009.** Vast  
851 underestimation of Madagascar's biodiversity evidenced by an integrative amphibian  
852 inventory. *Proceedings of the National Academy of Sciences of the United States of*  
853 *America* **106**: 8267-8272.
- 854 **Wallace AR. 1869.** *The Malay Archipelago: the land of the orang-utan and the bird of paradise;*  
855 *a narrative of travel, with studies of man and nature.* Courier Corporation.
- 856 **Warren BH, Simberloff D, Ricklefs RE, Aguilée R, Condamine FL, Gravel D, Morlon H,**  
857 **Mouquet N, Rosindell J, Casquet J, Conti E, Cornuault J, Fernandez-Palacios JM,**  
858 **Hengl T, Norder SJ, Rijdsdijk KF, Sanmartin I, Strasberg D, Triantis KA, Valente LM,**  
859 **Whittaker RJ, Gillespie RG, Emerson BC, Thebaud C. 2015.** Islands as model systems  
860 in ecology and evolution: prospects fifty years after MacArthur-Wilson. *Ecology*  
861 *Letters* **18**: 200-217.
- 862 **Whittaker RJ, Fernández-Palacios JM. 2007.** *Island biogeography: Ecology, evolution, and*  
863 *conservation.* OUP Oxford.
- 864 **Woodroffe SA, Long AJ, Milne GA, Bryant CL, Thomas AL. 2015.** New constraints on late

- 865           Holocene eustatic sea-level changes from Mahé, Seychelles. *Quaternary Science*  
866           *Reviews* **115**: 1-16.
- 867   **Xia X. 2013.** DAMBE5: a comprehensive software package for data analysis in molecular  
868           biology and evolution. *Molecular Biology and Evolution* **30**: 1720-1728.
- 869   **Xia X, Xie Z, Salemi M, Chen L, Wang Y. 2003.** An index of substitution saturation and its  
870           application. *Molecular Phylogenetics and Evolution* **26**: 1-7.
- 871   **Zhang J, Kapli P, Pavlidis P, Stamatakis A. 2013.** A general species delimitation method with  
872           applications to phylogenetic placements. *Bioinformatics* **29**: 2869-2876.
- 873   **Zoological Society of London. 2015.** EDGE of Existence Programme.  
874           <https://www.edgeofexistence.org/species/species-category/amphibians/> Accessed  
875           14<sup>th</sup> October 2018.

876 **Table 1** Sequenced gene fragments and summary statistics for analysed loci from *Sooglossus*  
 877 and *Sechellophryne* spp. tissue samples. Mitochondrial DNA = 16S rRNA (16s), cytochrome b  
 878 (*cytb*); nuclear DNA = proopiomelanocortin (*pomc*), recombination activating genes (*rag*) 1  
 879 and 2, rhodopsin exon 1 (*rho*). Data incorporates 16s sequence data obtained from GenBank  
 880 (superscript denotes no. of GenBank samples included in total). Dash (-) indicates sequence  
 881 data not obtained. N=sample size; bp=base pairs; Pi=parsimony informative sites; V=variable  
 882 sites;  $\pi$ =nucleotide diversity.

Species	Island	16s	<i>cytb</i>	<i>pomc</i>	<i>rag1</i>	<i>rag2</i>	<i>rho</i>
<i>So. sechellensis</i>	Mahé	76 <sup>(6)</sup>	16	10	19	59	18
	Silhouette	21	12	9	15	20	13
	Praslin	62 <sup>(15)</sup>	11	11	25	51	19
<i>So. thomasseti</i>	Mahé	17	7	6	11	15	7
	Silhouette	12	2	2	10	12	2
<i>Se. gardineri</i>	Mahé	15	4	7	10	15	11
	Silhouette	12	-	1	3	10	3
<i>Se. pipilodryas</i>	Silhouette	2 <sup>(1)</sup>	1	1	1 <sup>(1)</sup>	2 <sup>(1)</sup>	1
<i>N</i>		217	53	47	94	184	74
<i>bp</i>		532	549	348	383	521	279
<i>Pi</i>		111	154	31	22	57	13
<i>V</i>		119	184	42	32	76	15
$\pi$		0.0557	0.1113	0.0312	0.0169	0.0232	0.0043

**Table 2** Between taxa *16s* distance matrix for the Sooglossidae. Lower diagonal: uncorrected *p*-distance; upper diagonal: corrected Jukes-Cantor *p*-distance (Jukes & Cantor, 1969).

*Sechellophryne gardineri* = Sg; *Se. pipilodryas* = Sp; *Sooglossus sechellensis* = Ss; *So. thomasseti* = St.

	<b>Sg</b>	<b>Sp</b>	<b>Ss</b>	<b>St</b>
Sg		0.0704	0.1435	0.1346
Sp	0.0672		0.1555	0.1447
Ss	0.1306	0.1404		0.0608
St	0.1232	0.1316	0.0584	



**Table 3** Between population *16s* *p*-distance distance matrix for the Sooglossidae. Lower diagonal: uncorrected *p*-distance; upper diagonal: corrected Jukes-Cantor *p*-distance (Jukes & Cantor, 1969). *Sechellophryne gardineri* = Sg; *Se. pipilodryas* = Sp; *Sooglossus sechellensis* = Ss; *So. thomasseti* = St. M = Mahé, S = Silhouette, P = Praslin.

	<b>Sg-M</b>	<b>Sg-S</b>	<b>Sp</b>	<b>Ss-M</b>	<b>Ss-P</b>	<b>Ss-S</b>	<b>St-M</b>	<b>St-S</b>
Sg-M		0.0373	0.0701	0.1491	0.1477	0.1479	0.1407	0.1243
Sg-S	0.0364		0.0708	0.1395	0.1339	0.1402	0.1383	0.1313
Sp	0.0669	0.0675		0.1546	0.1551	0.1599	0.1473	0.1410
Ss-M	0.1352	0.1273	0.1397		0.0465	0.0399	0.0577	0.0622
Ss-P	0.1341	0.1226	0.1401	0.0451		0.0205	0.0647	0.0623
Ss-S	0.1342	0.1279	0.1440	0.0389	0.0202		0.0556	0.0572
St-M	0.1283	0.1263	0.1337	0.0556	0.0620	0.0536		0.0209
St-S	0.1145	0.1205	0.1285	0.0597	0.0598	0.0551	0.0206	

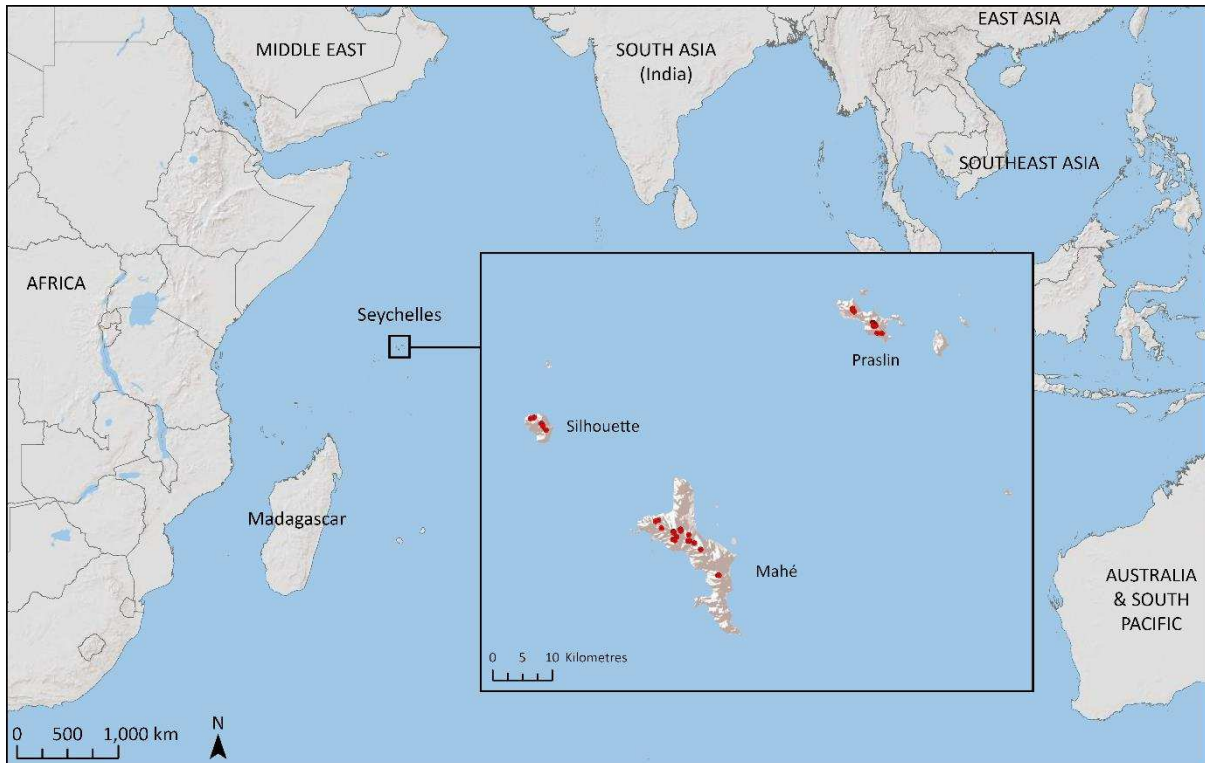


**Figure 1** Seychelles archipelago and the surrounding geographic regions of the Indian Ocean, inset with the inner islands of Mahé, Praslin, and Silhouette—the only locations where the Sooglossidae (Noble, 1931) are found. *Sooglossus sechellensis* (Boettger, 1896), *So. thomasseti* (Boulenger, 1909), and *Sechellophryne gardineri* (Boulenger, 1911) are sympatric on Mahé and Silhouette, with the addition of *Se. pipilodryas* (Gerlach & Willi, 2002) on Silhouette. *Sooglossus sechellensis* is the only sooglossid to occur on Praslin. Red circles indicate sampling localities and associated geographic data used to test for the effects of isolation by distance.

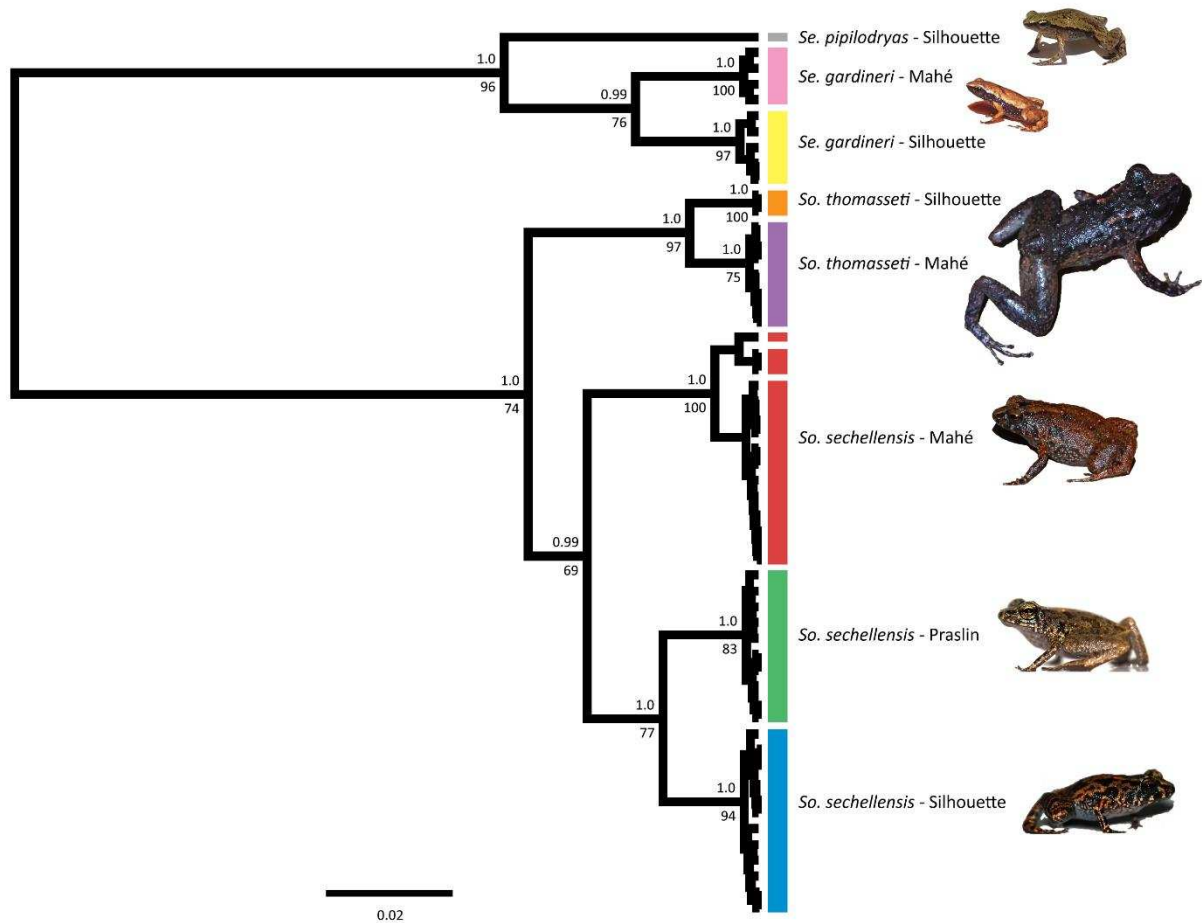


**Figure 2** Bayesian inferred mitochondrial DNA phylogeny of Seychelles Sooglossidae. Support values are shown as Bayesian posterior probabilities (PP: above branches) and maximum likelihood bootstrap values (BS: below branches). Scale bar indicates substitutions per site. Vertical coloured bars adjacent to branch tips correspond to the ten population/species boundaries returned by the maximum likelihood partition in bPTP analysis. Colour coding identifies the island lineage of each species: *Sooglossus thomasseti* (Mahé – orange; Silhouette – purple) is the largest sooglossid; followed by *So. sechellensis* (Mahé – red; Praslin – green; Silhouette – blue), which is also the most widely geographically distributed; then *Sechellophryne pipilodryas* (Silhouette – grey); and the smallest in the family, *Sechellophryne gardineri* (Mahé – pink; Silhouette – yellow).

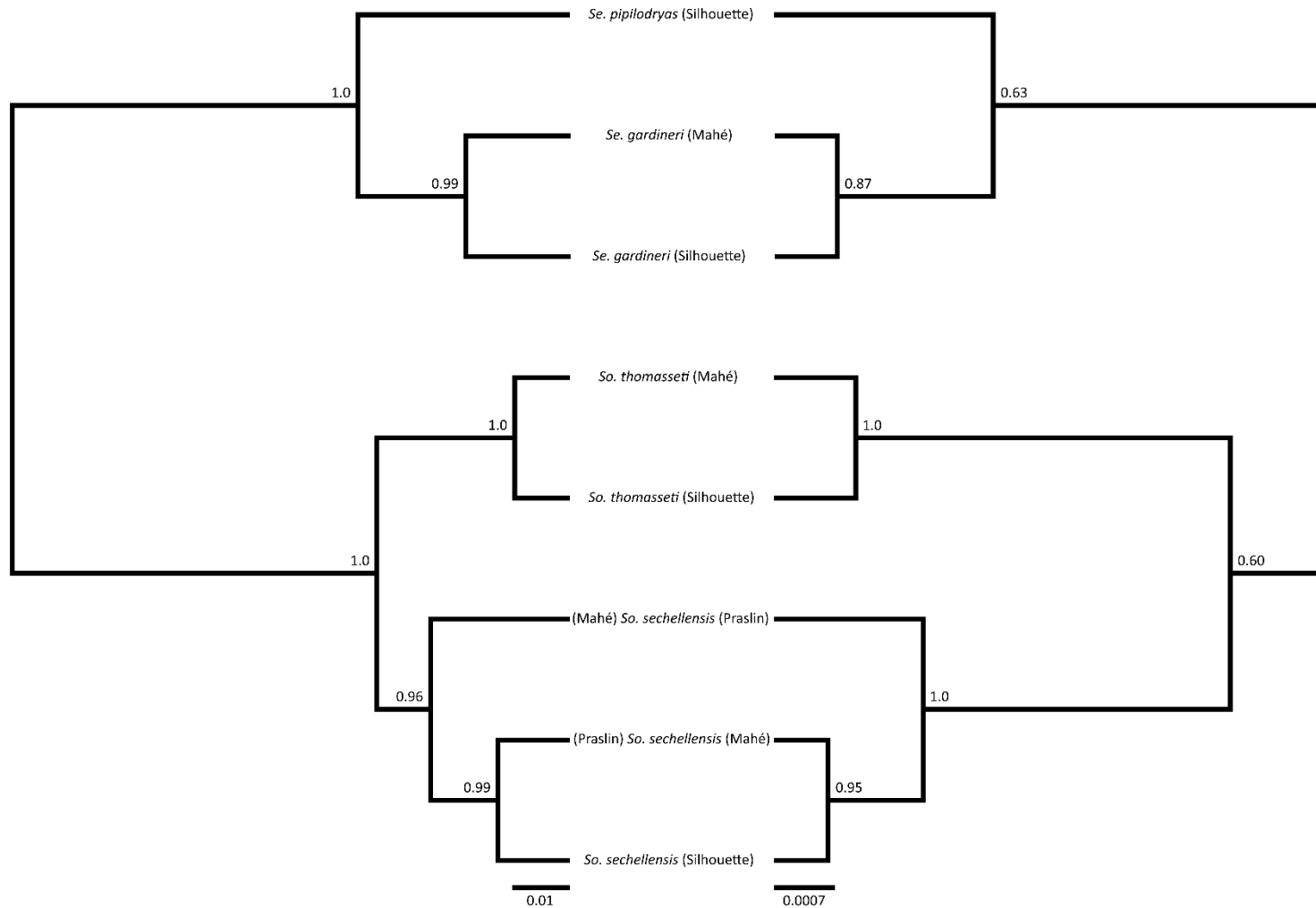


**Figure 3** \*BEAST generated mitochondrial (left) and nuclear (right) DNA species trees for the Sooglossidae. Branch numbers show PP support. The single topological disparity identifies Mahé *So. sechellensis* in the mtDNA species tree as sister to a clade comprised of those from Silhouette and Praslin, whereas in the nuDNA tree Silhouette and Mahé frogs form a clade sister to those from Praslin. Scale bar indicates substitutions per site.

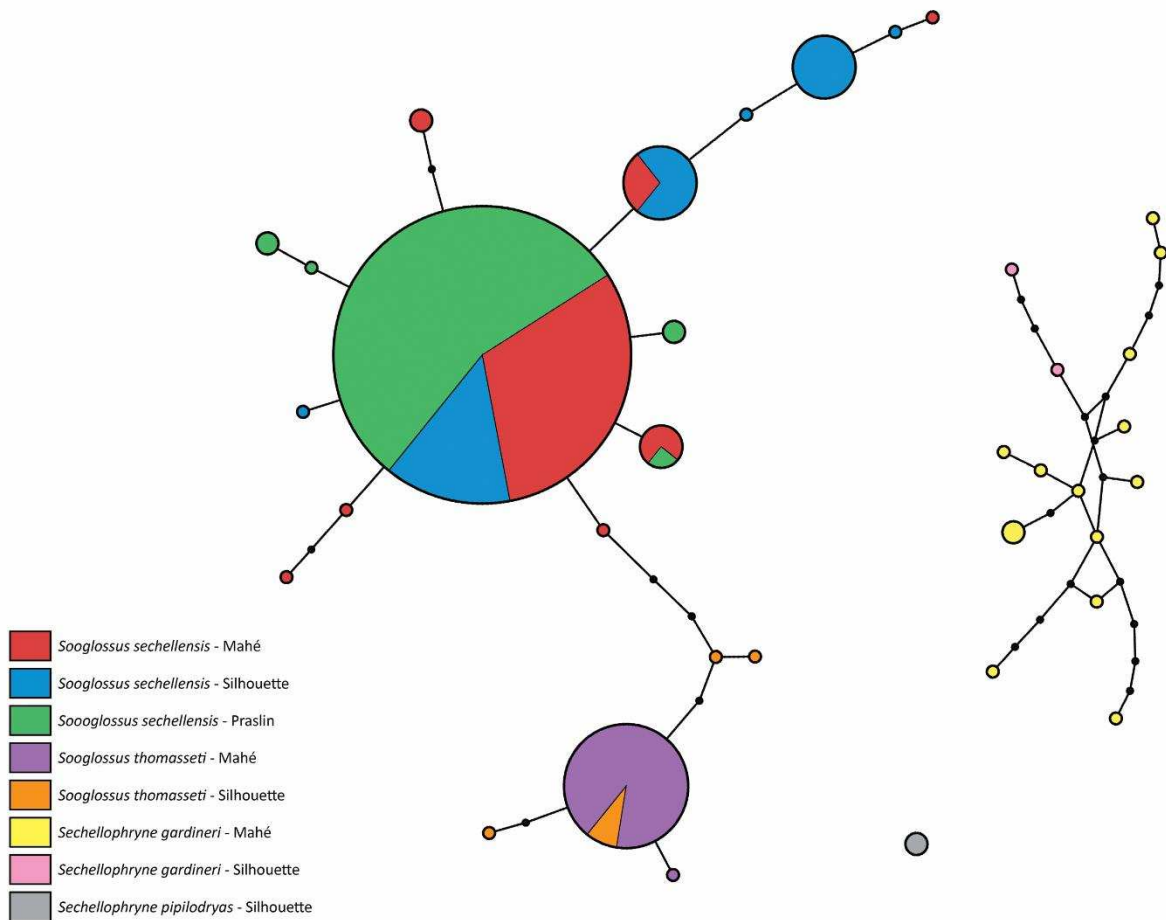


**Figure 4** Nuclear *pomc* DNA haplotype network for the Sooglossidae. Thirty-six haplotypes are present. Circle size is proportional to the frequency with which the haplotype was observed, i.e. larger circles represent high-frequency, shared haplotypes, smaller circles represent low-frequency/rare haplotypes. Closed black circles indicate mutational steps. Colours represent island populations (see legend/Fig. 2).

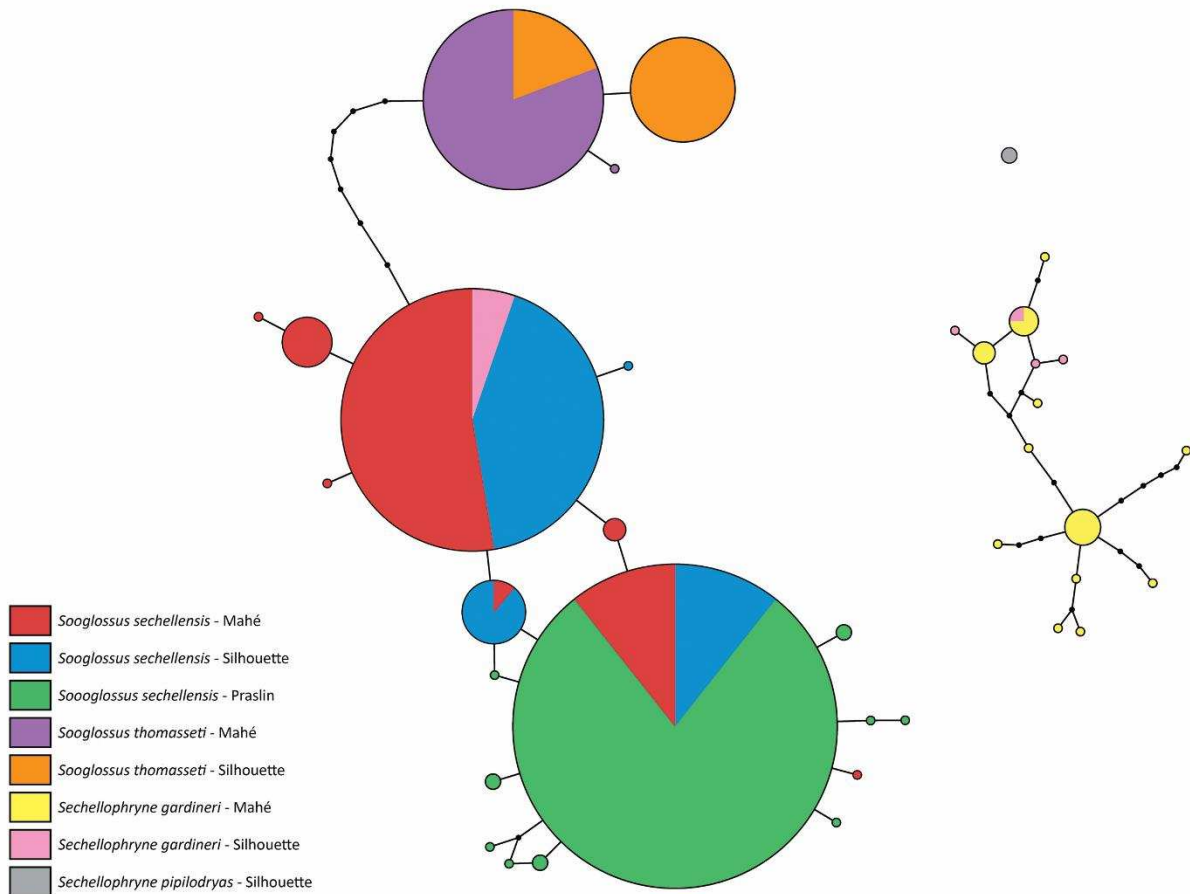


**Figure 5** Nuclear *rag1* DNA haplotype network for the Sooglossidae. Thirty-seven haplotypes are present. Circle size is proportional to the frequency with which the haplotype was observed, i.e. larger circles represent high-frequency, shared haplotypes, smaller circles represent low-frequency/rare haplotypes. Closed black circles indicate mutational steps. Colours represent island populations; colour coding follows that of previous figures.

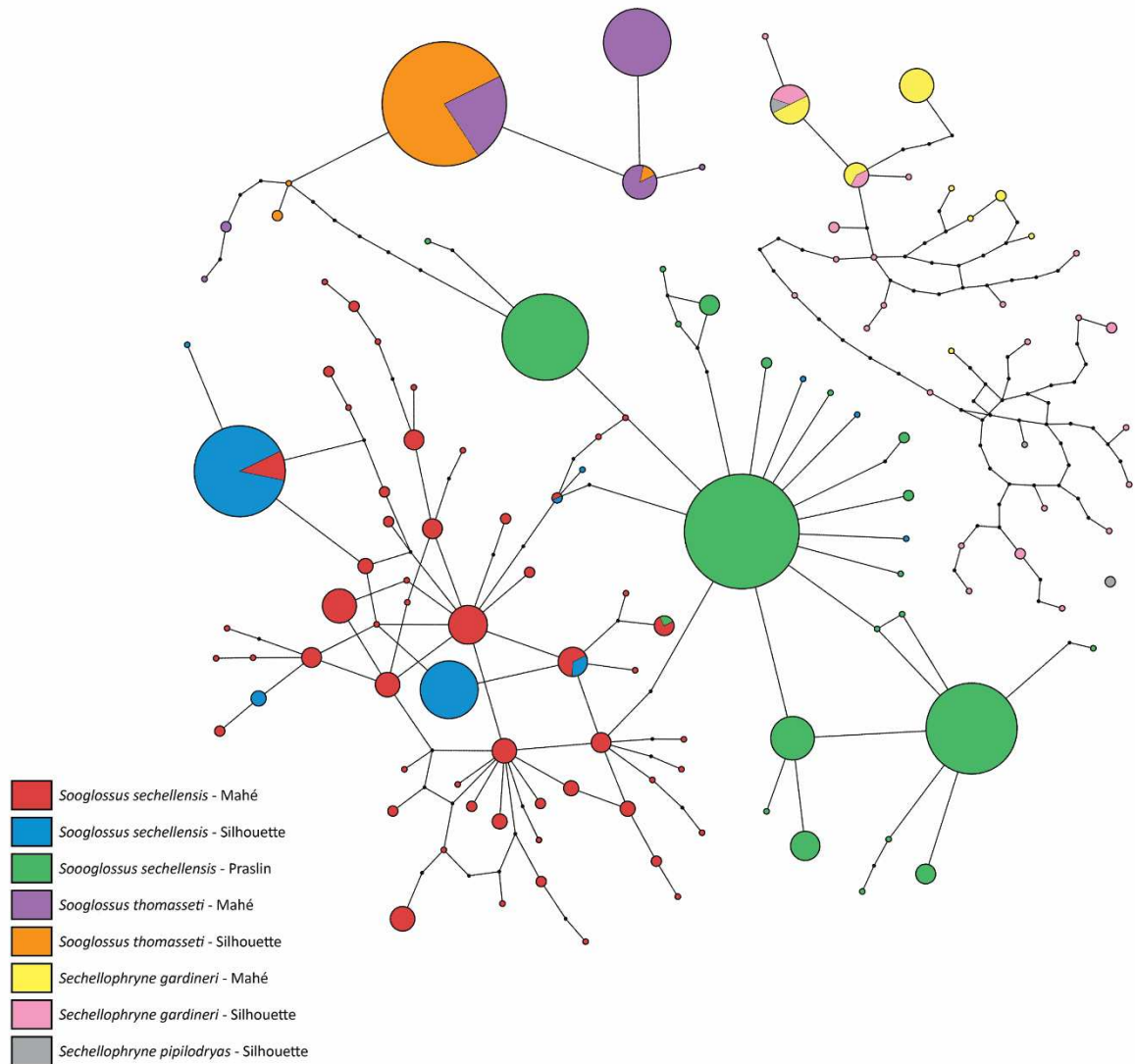


**Figure 6** Nuclear *rag2* DNA haplotype network for the Sooglossidae. One-hundred and twenty-three haplotypes are present. Circle size is proportional to the frequency with which the haplotype was observed, i.e. larger circles represent high-frequency, shared haplotypes, smaller circles represent low-frequency/rare haplotypes. Closed black circles indicate mutational steps. Colours represent island populations; colour coding follows that of previous figures.

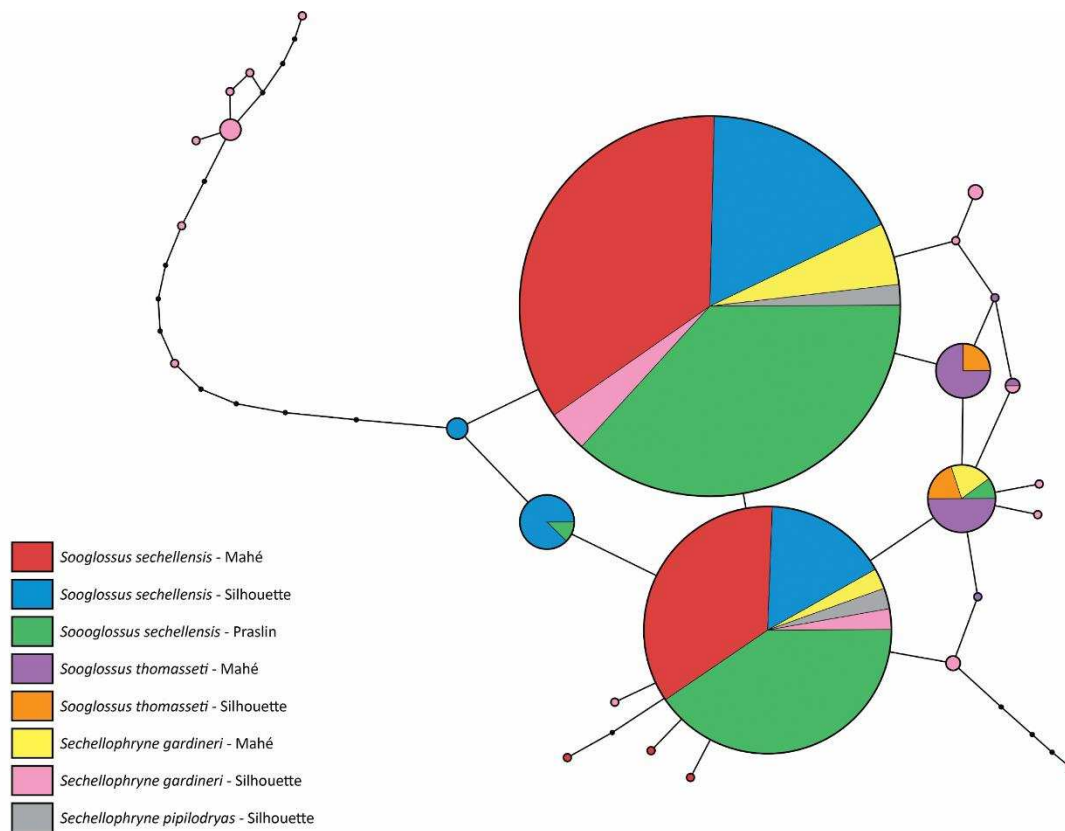


**Figure 7** Nuclear *rho* DNA haplotype network for the Sooglossidae. Twenty-six haplotypes are present. Circle size is proportional to the frequency with which the haplotype was observed, i.e. larger circles represent high-frequency, shared haplotypes, smaller circles represent low-frequency/rare haplotypes. Closed black circles indicate mutational steps. Colours represent island populations; colour coding follows that of previous figures.



## SUPPORTING INFORMATION

### Appendix S1

#### PCR cycling conditions & sequence data

Sequences from two mitochondrial (mtDNA) and four nuclear (nuDNA) loci were amplified via standard polymerase-chain reaction (PCR) with total reaction volumes of 10-42  $\mu$ l. Due to difficulty obtaining adequate DNA yields from such small biological samples (toe-clips from frogs regularly less than 10 mm SVL) volumes of template DNA varied between some reactions. For a 25  $\mu$ l reaction, reaction volumes consisted of 10.5  $\mu$ l ddH<sub>2</sub>O, 0.5  $\mu$ l each of forward and reverse primer (at a concentration of 25 pmol/ $\mu$ l), 12.5  $\mu$ l MyTaq HS Red mix™, and 1  $\mu$ l of template DNA. Details of primers used are shown in Table S1. Primer pairs developed for this study were generated using Primer-Blast (<https://www.ncbi.nlm.nih.gov/tools/primer-blast>). PCR cycling conditions were: denature at 95°C for 60 seconds (*16s*, *cytb*, *rag2*) or 94°C for 60 seconds (*pomc*, *rag1*, *rho*); followed by 35 (*16s*, *cytb*, *rag2*, *rho*) or 40 (*rag1*, *pomc*) cycles of denaturing at 95°C for 15 seconds (*16s*, *cytb*, *rag2*), or 94°C for 30 seconds (*pomc*, *rag1*, *rho*); annealing for 15 seconds at 53°C (*16s*, *cytb*), 59.5°C (*rag2*), or for 30 seconds at 56°C (*rag1*), 57°C (*pomc*), 60°C (*rho*); extending at 72°C for 10 seconds (*16s*, *cytb*), or 30 seconds (*pomc*, *rag1*, *rag2*, *rho*), with a final extension step of 72°C for 5 minutes. All *16s* samples were sequenced in both directions. Due to project constraints complimentary sequence data were not generated for all loci. Those obtained comprised the following: *cytb* = 17; *pomc* = 9; *rag1* = 2; *rag2* = 8; *rho* = 4. All sequences were cross-checked using the BLAST function in MEGA6 (Tamura, Stecher, Peterson, Filipski, & Kumar, 2013) and compared against sequences generated by this study. Ambiguous bases were coded accordingly.

**Table S1.1** Primers used for PCR amplification and sequencing.

Gene fragment	Primer	Sequence (5' – 3')
<i>16s</i>	16s A-L <sup>a</sup>	CGC CTG TTT ATC AAA AAC AT
	16s B-H <sup>a</sup>	CCG GTC TGA ACT CAG ATC ACG T
<i>cytb</i>	CBJ 10933 <sup>b</sup>	TAT GTT CTA CCA TGA GGA CAA ATA TC
	Cytb-c <sup>b</sup>	CTA CTG GTT GTC CTC CGA TTC ATG T
	CytbJL1f <sup>c</sup>	TAG ACC TCC CAA CCC CAT CC
	CytbJL1r <sup>c</sup>	GAG GTG TGT GTT AGT GGG GG
	CytbSGJL1f <sup>c</sup>	ACC GCT TTC GTA GGC TAT GT
	CytbSGJL1 <sup>c</sup>	GTG GAC GAA ATG ATA TTG CTC GT
<i>pomc</i>	POMCJLf <sup>c</sup>	GAC ATC GCC AAC TAT CCG GT
	POMCJLr <sup>c</sup>	AAG TGT TGT CCC CCG TGT TT
	POMCJL2f <sup>c</sup>	AAA CAC GGG GGA CAA CAC TT
	POMCJL2r <sup>c</sup>	CTT CTG AGT CGA CAC CAG GG
<i>rag1</i>	RAG1B <sup>d</sup>	ATG GGA GAT GTG AGT GAR AAR CA
	RAG1E <sup>d</sup>	TCC GCT GCA TTT CCR ATG TCR CA
<i>rag2</i>	RAG2 JG1-F <sup>c</sup>	TCG TCC TAC CAT GTT CAC CAA TGA GT
	RAG2 JG1-R <sup>c</sup>	TCC TGT CCA ATC AGG CAG TTC CA
	RAG2JLSG1f <sup>c</sup>	CCA GCA GTG ACC AGC ATC TT
	RAG2JLSG1r <sup>c</sup>	CGC TGT CTC TTG GAC TGG TT
	RAG2JLSG2r <sup>c</sup>	CCG ACA ATG AGG AAC TCG CT
<i>rho</i>	Rhod1A <sup>e</sup>	ACC ATG AAC GGA ACA GAA GGY CC
	Rhod1D <sup>e</sup>	GTA GCG AAG AAR CCT TCA AMG TA

<sup>a</sup> Palumbi *et al.*, (1991)<sup>b</sup> Chiari *et al.*, (2004)<sup>c</sup> Developed for this study<sup>d</sup> Biju & Bossuyt, (2003)<sup>e</sup> Bossuyt & Milinkovitch, (2000)

**Table S1.2** GenBank derived sequence data used in this study. Codes indicate Genbank accession numbers. Identical codes in adjacent columns for *Ascaphus truei* and *Leiopelma archeyi* represent sampling of independent sections of the mitochondrial genome of the same accessioned data.

<b>Species</b>	<b>16s</b>	<b>cytb</b>	<b>rag1</b>	<b>rag2</b>
<i>Ascaphus truei</i>	AJ871087	AJ871087	-	-
<i>Leiopelma archeyi</i>	NC_014691	NC_014691	-	-
<i>Sechellophryne pipilodryas</i>	DQ872918	-	DQ872922	DQ872912
<i>Sooglossus sechellensis</i>	JF784361	-	-	-
<i>Sooglossus sechellensis</i>	JF784362	-	-	-
<i>Sooglossus sechellensis</i>	JF784363	-	-	-
<i>Sooglossus sechellensis</i>	JF784364	-	-	-
<i>Sooglossus sechellensis</i>	JF784365	-	-	-
<i>Sooglossus sechellensis</i>	JF784366	-	-	-
<i>Sooglossus sechellensis</i>	JF784367	-	-	-
<i>Sooglossus sechellensis</i>	JF784368	-	-	-
<i>Sooglossus sechellensis</i>	JF784370	-	-	-
<i>Sooglossus sechellensis</i>	JF784371	-	-	-
<i>Sooglossus sechellensis</i>	JF784372	-	-	-
<i>Sooglossus sechellensis</i>	JF784373	-	-	-
<i>Sooglossus sechellensis</i>	JF784374	-	-	-
<i>Sooglossus sechellensis</i>	JF784376	-	-	-
<i>Sooglossus sechellensis</i>	JF784377	-	-	-
<i>Sooglossus sechellensis</i>	JF784378	-	-	-
<i>Sooglossus sechellensis</i>	JF784379	-	-	-
<i>Sooglossus sechellensis</i>	JF784380	-	-	-
<i>Sooglossus sechellensis</i>	JF784381	-	-	-
<i>Sooglossus sechellensis</i>	JF784382	-	-	-
<i>Sooglossus sechellensis</i>	JF784383	-	-	-

**Table S1.3** Partitioning schemes and substitution models selected by PartitionFinder v1.1.1 (Lanfear *et al.*, 2012) using the AIC criterion for Bayesian (BEAST2/\*BEAST) analyses. Codon positions in parentheses.

	<b>Partitioning scheme</b>	<b>Substitution model</b>
mtDNA	<i>16s</i> , <i>cytb</i> (1)	GTR+I+G
	<i>cytb</i> (2)	TrN+I
	<i>cytb</i> (3)	TrN+G
nuDNA	<i>pomc</i> (1-3)	TrN+I+G
	<i>rag1</i> (1-3)	TrN+I+G
	<i>rag2</i> (1-3)	TrN+I+G
	<i>rho</i> (1-3)	TrN+I+G

**Table S1.4** Taxa used as composites in \*BEAST analyses.

<b>Species</b>	<b>Ref.</b>	<b>Locus</b>	<b>Composite</b>
<i>Sechellophryne gardineri</i>	JMSG07	<i>rho</i>	JMSG09
<i>Sechellophryne pipilodryas</i>	DQ872922	<i>rag1</i>	JMSP01

**Table S1.5** Species/population boundaries inferred from Bayesian Poisson Tree Processes (bPTP) analysis. The BEAST2 mtDNA phylogeny was used as the input tree. Posterior probabilities (PP) of maximum likelihood and Bayesian analyses were identical. Populations are listed in node order as per the phylogeny (Fig. 2 in the main text).

<b>Species/population</b>	<b>Island</b>	<b>Sample reference</b>	<b>PP</b>
<i>Sechellophryne pipilodryas</i>	Silhouette	JMSP01	1.00
<i>Sechellophryne gardineri</i>	Mahé	CDSG01, MBSG04, LRSG03, MBSG02	0.97
<i>Sechellophryne gardineri</i>	Silhouette	DGSG01, JMSG01, JMSG05, JMSG07, JMSG10	0.75
<i>Sooglossus thomasseti</i>	Silhouette	GBST01, JMST06	0.99
<i>Sooglossus thomasseti</i>	Mahé	CDST02, CRST01, MCST02, LMST01, MSST01, CDST01, MBST01	0.98
<i>Sooglossus sechellensis</i>	Mahé	LRSS14	0.95
<i>Sooglossus sechellensis</i>	Mahé	LRSS01, MSSS02	0.95
<i>Sooglossus sechellensis</i>	Mahé	RSS01, LRSS02, LMSS01, SFSS02, CRSS14, CSS01, MSSS01, MCSS10, MBSS07, CRSS02, CRSS01, MBSS01	0.97
<i>Sooglossus sechellensis</i>	Praslin	VMSP16, CMSP01, CMSP07, CMSP02, FPSP03, FAT2, ZSP01, ZSP04, ZSP03, ZSP08	0.98
<i>Sooglossus sechellensis</i>	Silhouette	JMSS05, GBSS01, JMSS11, JMSS08, GBSS07, JMSS01, JMSS04, JMSS03, JMSS07, GBSS10, JMSS06, JMSS09	0.98

**Table S1.6** Population demographic tests for the Sooglossidae. Positive values of Tajima's  $D$  and Fu's  $F_S$  indicate stable population structure, balancing selection or recent population decrease; negative values indicate positive selection, or suggest evidence of recent population expansion. Tajima's  $D$  and  $R_2$  are interpreted as significant at  $P < 0.05$ , Fu's  $F_S$  at  $P < 0.02$ .

	<i>Sooglossus sechellensis</i>			<i>Sooglossus thomasseti</i>			<i>Sechellophryne gardineri</i>		
	Tajima's $D$	Fu's $F_S$	$R_2$	Tajima's $D$	Fu's $F_S$	$R_2$	Tajima's $D$	Fu's $F_S$	$R_2$
<i>16s</i>	2.36870	3.278	0.1621	3.10581	12.422	0.2512	2.24857	3.284	0.2073
	$P < 0.05$	$P > 0.02$	$P > 0.05$	$P < 0.01$	$P > 0.02$	$P > 0.05$	$P < 0.05$	$P > 0.02$	$P > 0.05$
<i>cytb</i>	1.71837	-1.421	0.1910	0.44661	3.394	0.1967	-0.55827	-0.361	0.1061
	$P > 0.05$	$P > 0.02$	$P > 0.05$	$P > 0.05$	$P > 0.02$	$P > 0.05$	$P > 0.05$	$P > 0.02$	$P < 0.05$
<i>pomc</i>	-1.40180	-8.378	0.0560	-1.21781	-1.557	0.0963	-0.64112	-10.089	0.1300
	$P > 0.05$	$P < 0.02$	$P > 0.05$	$P > 0.05$	$P > 0.02$	$P < 0.01$	$P > 0.05$	$P < 0.02$	$P > 0.05$
<i>rag1</i>	-1.21313	-7.542	0.0534	0.21337	0.346	0.1401	-0.13712	-0.421	0.1331
	$P > 0.05$	$P < 0.02$	$P > 0.05$	$P > 0.05$	$P > 0.02$	$P > 0.05$	$P > 0.05$	$P > 0.02$	$P > 0.05$
<i>rag2</i>	-1.77022	-82.555	0.0335	-0.12593	-1.420	0.1044	-0.65881	-8.246	0.0910
	$P < 0.05$	$P < 0.02$	$P < 0.05$	$P > 0.05$	$P > 0.02$	$P > 0.05$	$P > 0.05$	$P = 0.02$	$P > 0.05$
<i>rho</i>	-1.37952	-1.467	0.1000	0.65931	-0.801	0.1846	0.89497	-0.346	0.1582
	$P > 0.05$	$P > 0.02$	$P > 0.05$	$P > 0.05$	$P > 0.05$	$P > 0.05$	$P > 0.05$	$P > 0.02$	$P > 0.05$

**Table S1.7** Extended Bayesian Skyline Plot (EBSP) results for sooglossid populations. Results are the 95% highest posterior density (HPD) interval for population size changes from all loci in a combined analyses. Constant population size cannot be rejected if the 95% HPD interval includes 0. Plus sign (+) indicates population expansion. Low sample sizes can lead to unreliable EBSP results (Heller & Siegismund, 2013) and consistent ESS values were not obtained for the Silhouette population of *Se. gardineri* until we removed underrepresented loci (*pomc*, *rag1*, *rho*).

Island	<i>Sooglossus sechellensis</i>			<i>Sooglossus thomasseti</i>		<i>Sechellophryne gardineri</i>	
	Mahé	Praslin	Silhouette	Mahé	Silhouette	Mahé	Silhouette
Chain length	$3 \times 10^8$	$2 \times 10^8$	$5 \times 10^7$	$1 \times 10^8$	$7.5 \times 10^7$	$5 \times 10^7$	$5 \times 10^7$
EBSP	[0, 3]	[1, 3] <sup>+</sup>	[0, 3]	[0, 3]	[0, 3]	[0, 3]	[0, 2]



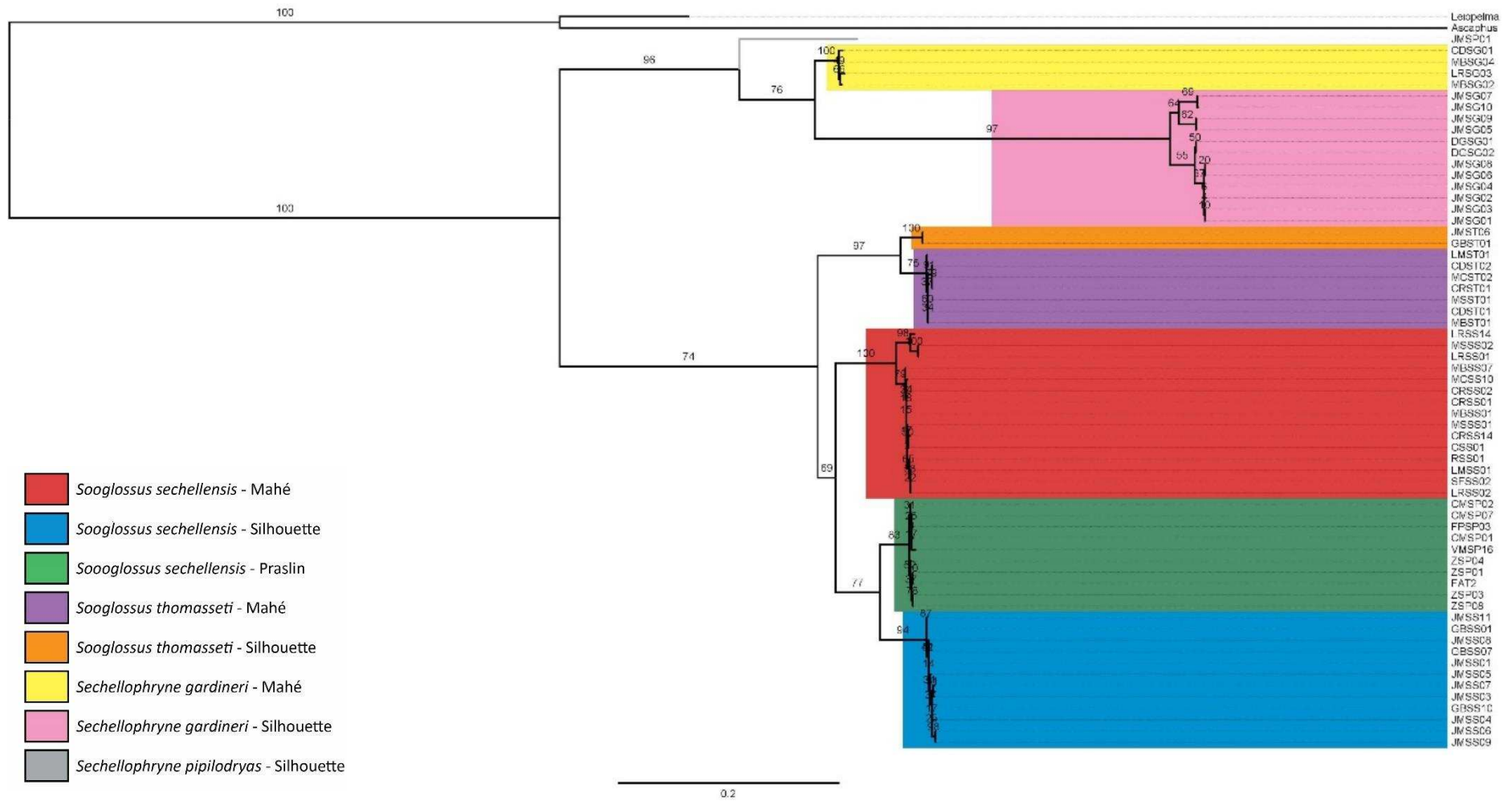


**Figure S1.1** Maximum likelihood inferred mitochondrial DNA phylogeny of the Sooglossidae. Leiopelemaoidea (*Leiopelema*+*Ascaphus*) rooted outgroup. Branch support is indicated by maximum likelihood bootstrap (BS) values. Scale bar indicates substitutions per site.

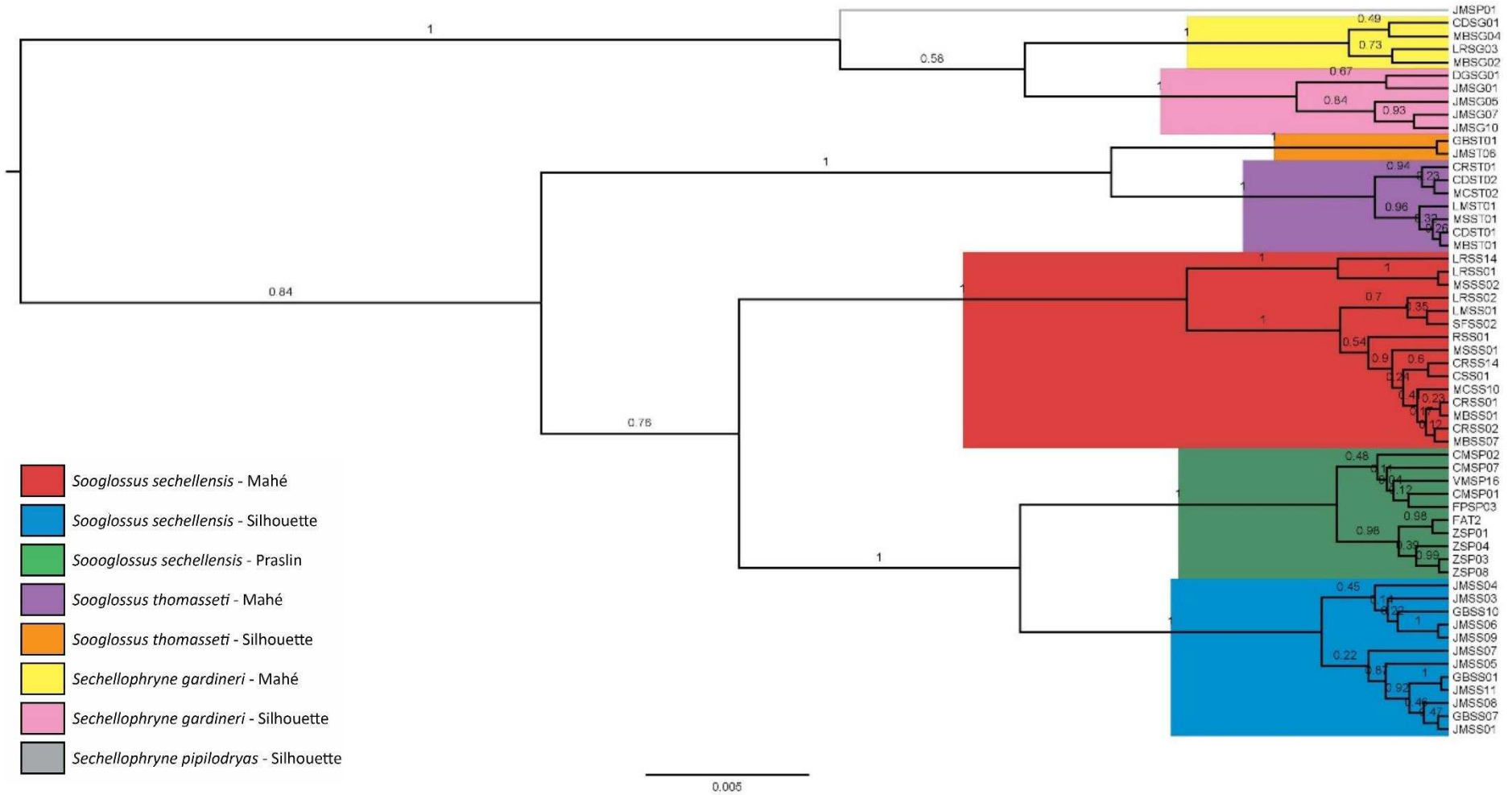


**Figure S1.2** Bayesian inferred mitochondrial DNA phylogeny of the Sooglossidae using the Yule tree prior in BEAST2. Branch support is indicated by Bayesian Posterior Probabilities (PP). Scale bar indicates substitutions per site.

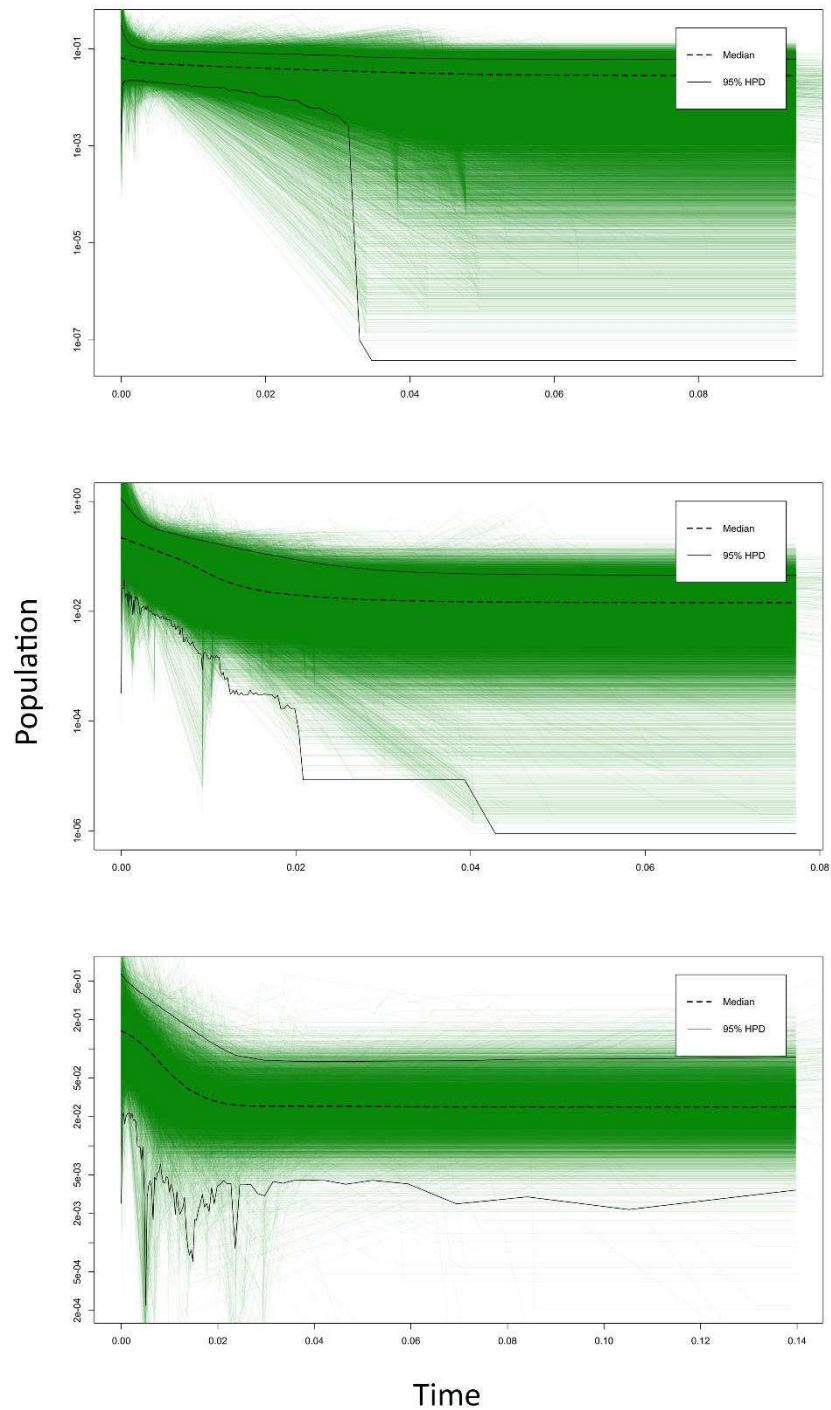


**Figure S1.3** Extended Bayesian Skyline Plots of population size through time for *Sooglossus sechellensis*. The full view of the posterior all of the samples that are summarised by the median and 95% HPD interval are shown for the Mahé (top), Praslin (centre), and Silhouette (bottom) populations. The Praslin frogs are the only sooglossid population to reject a constant population size. EBSP analyses comprised all six loci. Time on x-axis in millions of years. Population size on y-axis in millions of years assuming a generation time of one year.

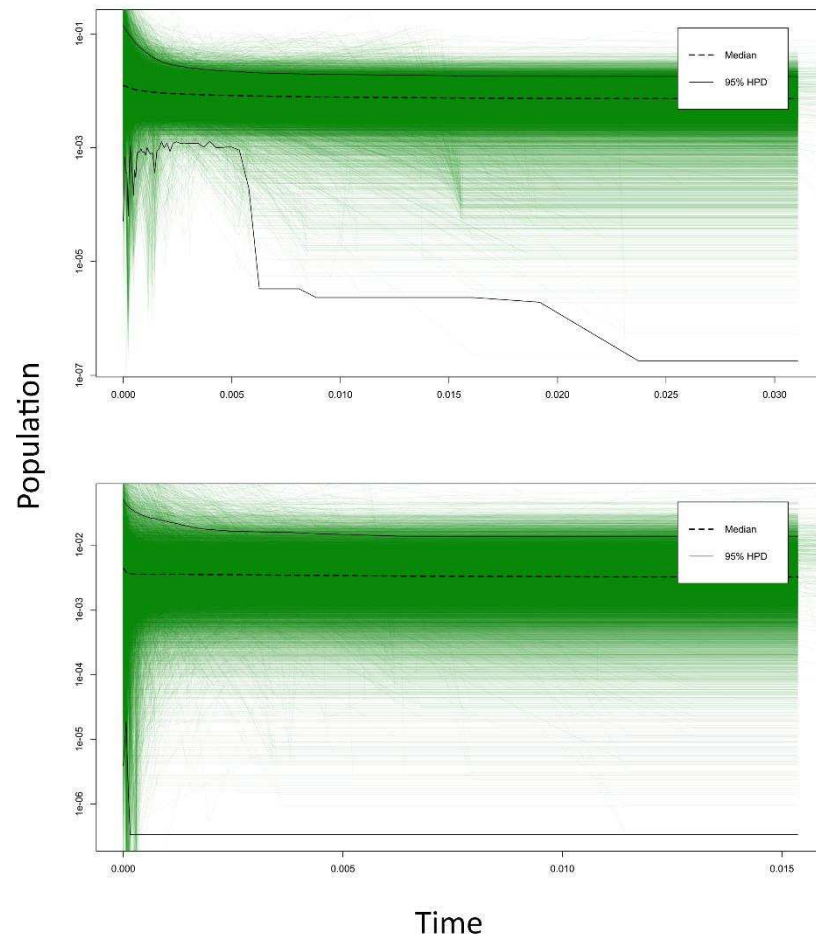


**Figure S1.4** Extended Bayesian Skyline Plots of population size through time for *Sooglossus thomasseti*. The full view of the posterior all of the samples that are summarised by the median and 95% HPD interval are shown for the Mahé (top) and Silhouette (bottom) populations. EBSP analyses comprised all six loci. Time on x-axis in millions of years. Population size on y-axis in millions of years assuming a generation time of one year.

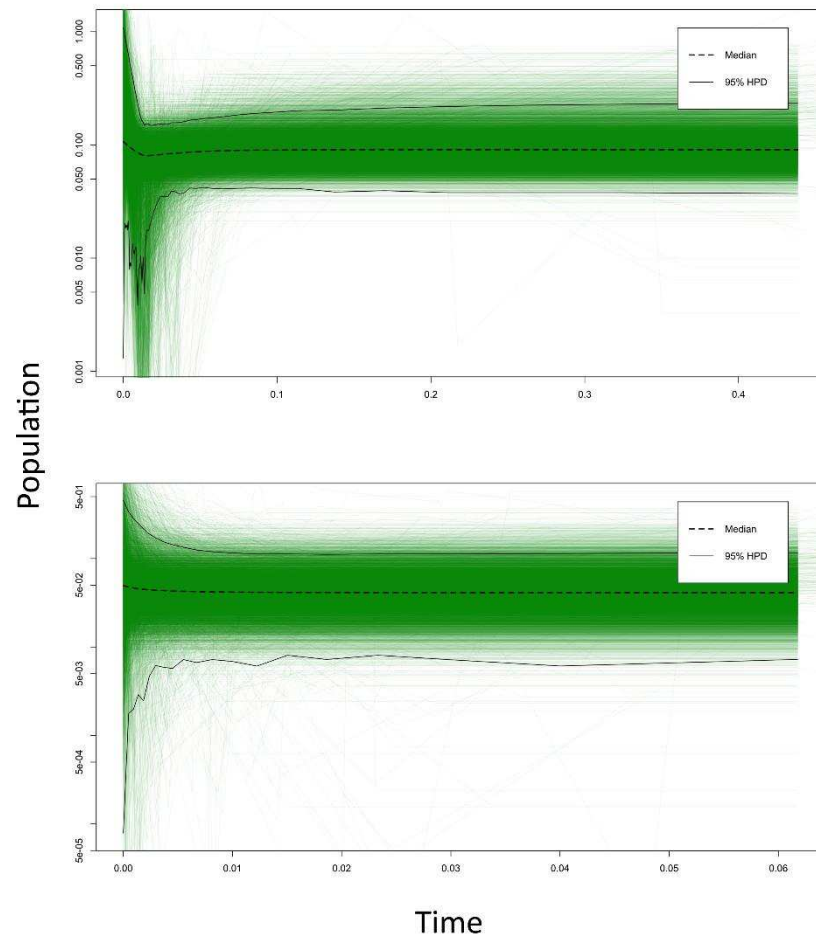


**Figure S1.5** Extended Bayesian Skyline Plots of population size through time for *Sechellophryne gardineri*. The full view of the posterior all of the samples that are summarised by the median and 95% HPD interval are shown for the Mahé (top) and Silhouette (bottom) populations. EBS analyses of the Mahé population comprised all six loci. Analyses of the Silhouette population comprised two loci (*16s*, *rag2*). Time on x-axis in millions of years. Population size on y-axis in millions of years assuming a generation time of one year

## References

- Biju SD, Bossuyt F. 2003.** New frog family from India reveals an ancient biogeographical link with the Seychelles. *Nature* **425**: 711-714.
- Bossuyt F, Milinkovitch MC. 2000.** Convergent adaptive radiations in Madagascan and Asian ranid frogs reveal covariation between larval and adult traits. *Proceedings of the National Academy of Sciences* **97**: 6585-6590.
- Chiari Y, Vences M, Vieites DR, Rabemananjara F, Bora P, Ramilijaona Ravoahangimalala O, Meyer A. 2004.** New evidence for parallel evolution of colour patterns in Malagasy poison frogs (*Mantella*). *Molecular Ecology* **13**: 3763-3774.
- Heller R, Chikhi L, Siegismund HR. 2013.** The confounding effect of population structure on Bayesian skyline plot inferences of demographic history. *PLoS One* **8**: e62992.
- Jukes TH, Cantor CR. 1969.** Evolution of protein molecules. In: Munro HN, ed. *Mammalian protein metabolism*. New York.: Academic Press. 21-132.
- Lanfear R, Calcott B, Ho SY, Guindon S. 2012.** Partitionfinder: combined selection of partitioning schemes and substitution models for phylogenetic analyses. *Molecular Biology and Evolution* **29**: 1695-1701.
- Palumbi S, Martin A, Romano S, McMillan WO, Stice L, Grabowski G. 1991.** *The simple fool's guide to PCR*. Dept. of Zoology and Kewalo Marine Laboratory, University of Hawaii: Honolulu, HI.
- Tamura K, Stecher G, Peterson D, Filipowski A, Kumar S. 2013.** MEGA6: Molecular Evolutionary Genetics Analysis version 6.0. *Molecular Biology and Evolution* **30**: 2725-2729.